

SafEDMD: A certified learning architecture tailored to data-driven control of nonlinear dynamical systems

Robin Strässer¹, Manuel Schaller², Karl Worthmann², Julian Berberich¹, Frank Allgöwer¹

Abstract

The Koopman operator serves as the theoretical backbone for machine learning of dynamical control systems, where the operator is heuristically approximated by extended dynamic mode decomposition (EDMD). In this paper, we propose Stability- and certificate-oriented EDMD (SafEDMD): a novel EDMD-based learning architecture which comes along with rigorous certificates, resulting in a reliable surrogate model generated in a data-driven fashion. To ensure trustworthiness of SafEDMD, we derive proportional error bounds, which vanish at the origin and are tailored for control tasks, leading to certified controller design based on semi-definite programming. We illustrate the developed machinery by means of several benchmark examples and highlight the advantages over state-of-the-art methods.

1. INTRODUCTION

Extended dynamic mode decomposition (EDMD; [1]) is one of the most popular machine learning algorithms to learn highly nonlinear dynamical (control) systems from data. Its applications range from climate forecasting [2], over electrocardiography [3] to quantum mechanics [4], cryptography [5], and nonlinear fluid dynamics [6]. The strength of EDMD lies in its analytical foundation by means of the Koopman operator, which *propagates* observable functions (e.g., measurement sensors) along the flow of the underlying dynamical system. As the Koopman operator acts linearly on observables, EDMD leverages tools from regression to efficiently learn this linear object on a finite-dimensional set of observables, which renders the implementation of this learning algorithm relatively straightforward. Moreover, advanced tools from operator theory and linear regression enable certification of this machine learning algorithm [7], [8]. For control tasks, in particular in safety-critical applications, such certificates are key [9]. The EDMD algorithm can be extended to control systems in order to take advantage of the reliability and strong analytical foundation. Two algorithms are predominantly used throughout the literature, namely EDMDc [10], [11] and bilinear EDMD [12], [13], where a linear and bilinear model is learned, respectively. As such, EDMD with control has been extensively and successfully used in various applications, see [14] and the references therein.

The reliable control of complex systems based on EDMD requires certificates on the learning algorithm. To this end, [15] proved convergence of EDMD to the Koopman operator in the infinite-data limit. First finite-data error bounds, including bilinear EDMD for control systems, were proven in [16]. The error bounds in these work, however, are global in the sense that the error does not vanish at the origin, which prevents a straightforward application of standard control methods.

F. Allgöwer is thankful that this work was funded by the Deutsche Forschungsgemeinschaft (DFG, German Research Foundation) under Germany's Excellence Strategy – EXC 2075 – 390740016 and within grant AL 316/15-1 – 468094890. K. Worthmann gratefully acknowledges funding by the German Research Foundation (DFG; project number 507037103). R. Strässer thanks the Graduate Academy of the SC SimTech for its support.

¹R. Strässer, J. Berberich, and F. Allgöwer are with the Institute for Systems Theory and Automatic Control, University of Stuttgart, 70550 Stuttgart, Germany (email: {robin.straesser, julian.berberich, frank.allgower}@ist.uni-stuttgart.de)

²M. Schaller and K. Worthmann are with the Institute for Mathematics, Technische Universität Ilmenau, 99693 Ilmenau, Germany (e-mail: {manuel.schaller, karl.worthmann}@tu-ilmenau.de).

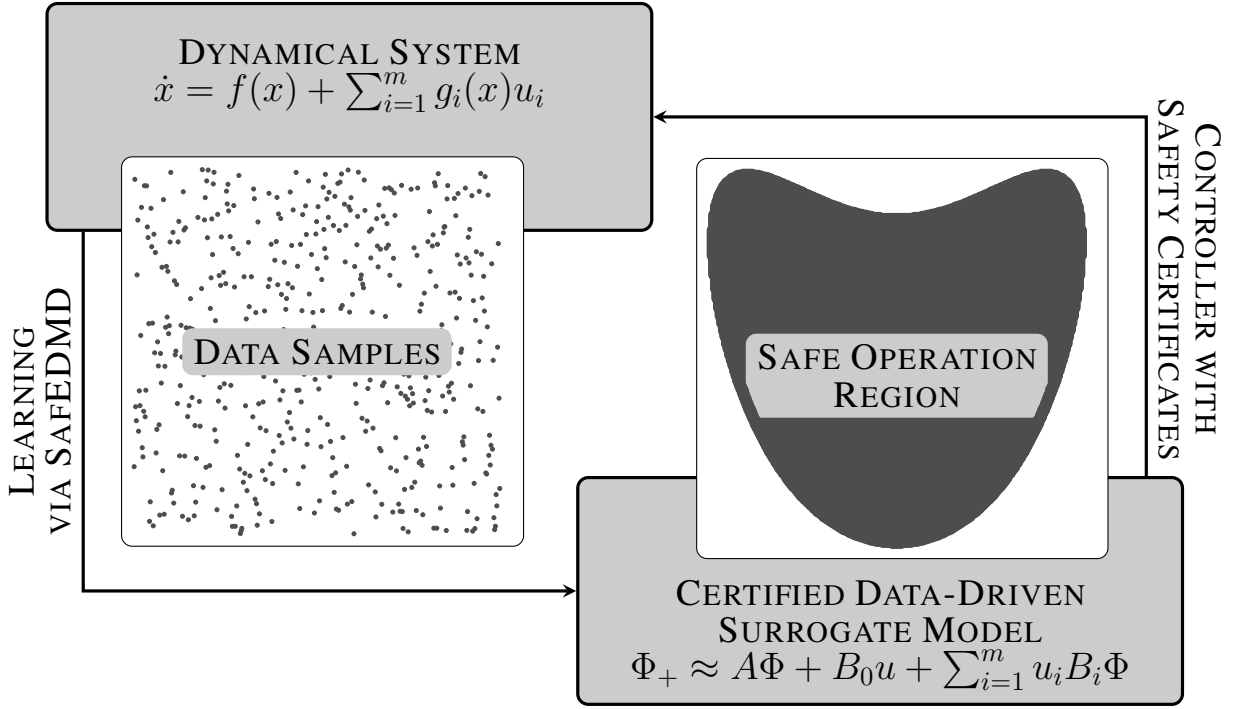


Fig. 1. Illustration of the proposed learning architecture SafEDMD tailored for certified data-driven control. The proposed approach first learns a bilinear surrogate model of the unknown nonlinear system based on data samples along with rigorous error bounds. Next, a controller is designed which exploits the model and the guaranteed error bounds to reliably control the nonlinear system in a safe operating region.

In this work, we present **Stability- and certificate-oriented EDMD (SafEDMD)** - a learning architecture with rigorous certificates, which is tailored to data-driven control of nonlinear systems. The architecture relies on a structured EDMD algorithm to learn a bilinear surrogate model of a nonlinear system based on data samples. To enable reliable controller design, SafEDMD is accompanied by bounds on its approximation error which, in contrast to existing results, vanish at the origin. This enables the design of safe controllers, which we illustrate with the exemplary control objective of stabilization in a safe operating region. The central idea of the proposed architecture is connected to [17], [18]. The key difference is that the proposed approach handles the Koopman operator directly in the discrete time domain using sampled data of the system. On the contrary, [17], [18] work with the corresponding *generator*, requiring time derivative data of system trajectories, which are very hard to obtain and typically significantly noisier in practice. To the best of our knowledge, the proposed approach is the first to control unknown nonlinear systems based on derivative-free data using the Koopman operator while giving rigorous stability certificates.

The overall approach is illustrated in Fig. 1 with the main contributions summarized as follows:

- (1) We propose SafEDMD – a novel certified and highly efficient architecture for machine learning with EDMD particularly suited for control tasks.
- (2) We rigorously derive certified error bounds tailored to controller design.
- (3) To illustrate the applicability of the proposed learning architecture and its error bounds, we exemplarily design a feedback controller and provide a certificate for the successful completion of the stabilization task.
- (4) We illustrate the methodology with various examples, highlighting scenarios where the proposed architecture allows to successfully learn and control unknown nonlinear systems whereas existing methods fail.

The paper is organized as follows. In Section 2, we recall the notion of the Koopman operator and its representation of nonlinear dynamical systems. Section 3 describes the framework SafEDMD introducing a certified learning architecture tailored to data-driven control. Section 4 illustrates the applicability of

SafEDMD for control tasks, where we design a certified data-driven feedback controller. Finally, Section 5 validates our proposed learning architecture as well as the controller design in numerical experiments.

2. THE KOOPMAN OPERATOR AS FOUNDATION FOR CERTIFIABLE LEARNING OF DYNAMICAL SYSTEMS

In the following, we briefly recap the necessary background on the Koopman operator and its representation of nonlinear dynamical systems in Section 2.1. Then, in Section 2.2, we discuss a sampled-data Koopman representation in preparation for the proposed certified learning scheme.

2.1. Koopman representation of nonlinear dynamical systems

Throughout the paper, we consider *unknown* nonlinear control-affine systems of the form

$$\dot{x}(t) = f(x(t)) + \sum_{i=1}^m g_i(x(t))u_i(t), \quad (1)$$

where $x(t) \in \mathbb{R}^n$ denotes the state at time $t \geq 0$ and the sufficiently smooth control function $u : [0, \infty) \rightarrow \mathbb{R}^m$ serves as an input. The map $f : \mathbb{R}^n \rightarrow \mathbb{R}^n$ is called drift, while $g_i : \mathbb{R}^n \rightarrow \mathbb{R}^n$, $i \in [m]$, are called input maps¹. For an initial condition $x(0) = \hat{x} \in \mathbb{R}^n$ and a control function u , we denote the solution of (1), provided it exists, at time $t \geq 0$ by $x(t; \hat{x}, u)$. We assume that $f(0) = 0$ holds, i.e., the origin is a controlled equilibrium for $u = 0$.

The Koopman operator \mathcal{K}_t^u introduced in [19] provides a powerful alternative representation of the nonlinear dynamical system (1) through the lens of observable functions given by, e.g., measurements in a particular application. More precisely, the Koopman operator \mathcal{K}_t^u corresponding to (1) with constant input $u(t) \equiv u \in \mathbb{U}$ for a compact set $\mathbb{U} \subseteq \mathbb{R}^m$ with $0 \in \text{int}(\mathbb{U})$ is defined as

$$(\mathcal{K}_t^u \varphi)(\hat{x}) = \varphi(x(t; \hat{x}, u)) \quad (2)$$

for all $t \geq 0$, $\hat{x} \in \mathbb{X}$, $\varphi \in L^2(\mathbb{X}, \mathbb{R})$, where $\mathbb{X} \subseteq \mathbb{R}^n$ is a compact set and the real-valued functions φ are called *observables*.² As the Koopman operator \mathcal{K}_t^u is an infinite-dimensional, but *linear* operator on observable functions φ , it enables the use of powerful data-driven techniques for learning such as, e.g., linear regression.

As shown in, e.g., in [17], [21], [22], the Koopman operator \mathcal{K}_t^u inherits the control-affine structure of (1) *approximately*, i.e.,

$$\mathcal{K}_t^u \approx \mathcal{K}_t^0 + \sum_{i=1}^m u_i (\mathcal{K}_t^{e_i} - \mathcal{K}_t^0) \quad (3)$$

holds, where \mathcal{K}_t^0 and $\mathcal{K}_t^{e_i}$, $i \in [m]$, are the Koopman operators corresponding to the constant control functions $u \equiv 0$ and $u \equiv e_i$ with unit vectors e_i , $i \in [m]$, respectively.

The core of data-driven techniques leveraging the Koopman operator, such as EDMD as discussed later, is to learn the action of the Koopman operator on a subspace, called the *dictionary*. To this end, we define the dictionary $\mathbb{V} := \text{span}\{\phi_\ell\}_{\ell=0}^N$ representing the $(N+1)$ -dimensional subspace spanned by the chosen observables $\phi_0 \equiv 1$ and $\phi_\ell \in \mathcal{C}^2(\mathbb{R}^n, \mathbb{R})$ with $\phi_\ell(0) = 0$, $\ell \in [N]$. In particular, we choose the observables

$$\Phi(x) = [1 \quad x^\top \quad \phi_{n+1}(x) \quad \cdots \quad \phi_N(x)]^\top. \quad (4)$$

Note that

$$\|x\| \leq \|\Phi(x) - \Phi(0)\| \leq L_\Phi \|x\|, \quad (5)$$

¹In this paper, we use $[a : b] := \mathbb{Z} \cap [a, b]$ and $[b] := [1 : b]$.

²Here, we tacitly assumed invariance of \mathbb{X} under the flow such that the observable functions are defined on $x(t; \hat{x}, u)$ for all $\hat{x} \in \mathbb{X}$. This assumption can be relaxed by considering initial values contained in a tightened version of \mathbb{X} , see, e.g., [20] for details.

where the first inequality follows since Φ explicitly contains x , and the second inequality follows from local Lipschitz continuity due to $\Phi \in \mathcal{C}^2(\mathbb{R}^n, \mathbb{R}^N)$. Common choices for the observables Φ include monomials or radial basis functions such as, e.g., thin-plate splines. If prior knowledge about the system dynamics is available, suitable observables can often be inferred from the system dynamics, see, e.g., [23] or [24] for a novel approach to construct a dictionary tailored to robotic systems. Although not explicitly considered in this paper, the observables ϕ_ℓ , $\ell \in [n+1, N]$ can also be learned via a neural network (NN). Parametrizing Φ by an NN increases the expressiveness and allows finding suitable nonlinear observables ϕ_ℓ for the underlying system dynamics (1), see, e.g., [25]. Here, the assumed Lipschitz continuity in (5) of the learned NN can be ensured by design [26].

Throughout the paper, we assume invariance of the dictionary \mathbb{V} w.r.t. the dynamics.

Assumption 2.1 (Invariance of \mathbb{V}). For any $\phi \in \mathbb{V}$, the relation $\phi(x(t; \hat{x}, u)) \in \mathbb{V}$ holds for all $u(t) \equiv \hat{u} \in \mathbb{U}$, $\hat{x} \in \mathbb{X}$, and $t \geq 0$.

Assumption 2.1 is commonly employed for a Koopman-based representation of controlled systems. Conditions for the (approximate) satisfaction of this assumption are given by, e.g., [27]–[29]. We note that even if Assumption 2.1 does not hold, there are first works considering the resulting projection error [8], [30]. As a consequence of Assumption 2.1, the Koopman operator acts as a linear operator mapping the finite-dimensional dictionary to itself. With slight abuse of notation, we thus denote by \mathcal{K}_t^u its matrix representation.

2.2. Sampled-data Koopman representation

When controlling dynamical systems of the form (1), a direct implementation of a (piecewise) continuous control function $u : [0, \infty) \rightarrow \mathbb{R}^m$ is typically not feasible. Instead, a common strategy is to sample the system (1), e.g., equidistantly in time, and consider piecewise constant control inputs on each interval, i.e., $u(t) \equiv u_k \in \mathbb{U}$ holds for all $t \in [t_k, t_k + \Delta t)$ with sampling period $\Delta t > 0$ and $t_k = k\Delta t$, $k \in \mathbb{N}_0$. This leads to the discretized system representation

$$x_{k+1} = x_k + \int_{t_k}^{t_k + \Delta t} f(x(t)) + \sum_{i=1}^m g_i(x(t))(u_k)_i dt \quad (6)$$

with $x(t) = x(t; \hat{x}, u)$ and $x_k = x(t_k; \hat{x}, u)$. From (2) and Assumption 2.1, we deduce the discrete-time Koopman representation

$$\Phi(x_{k+1}) = \mathcal{K}_{\Delta t}^u \Phi(x_k). \quad (7)$$

Note that the evolution of $\Phi(x_k)$ allows to retrieve the underlying state x by projection due to the choice of the lifting function Φ in (4), such that $x = \begin{bmatrix} 0_{n \times 1} & I_n & 0_{n \times N-n} \end{bmatrix} \Phi(x)$ by definition.

3. SAFEDMD: A CERTIFIED LEARNING ARCHITECTURE TAILORED TO NONLINEAR DYNAMICAL SYSTEMS

In the following, we present a tailored learning architecture for nonlinear systems based on the Koopman operator particularly suited for certifiability in control tasks. Since the true nonlinear system dynamics are unknown, we leverage the linearity of the Koopman operator in the observables to learn a certifiable data-driven approximation. More precisely, we introduce a novel learning architecture called *SafEDMD*. This framework 1) learns a data-based bilinear surrogate model of the Koopman operator solely relying on linear regression and 2) ensures error certificates that allow the usage of the surrogate model for reliable control tasks, e.g., closed-loop stabilization.

In order to determine data-driven estimates of $\mathcal{K}_{\Delta t}^u$ for constant control inputs $u(t) \equiv \bar{u}$ for $\bar{u} \in \{0, e_1, \dots, e_m\}$, we consider data samples $\mathcal{D} = \{x_j^{\bar{u}}, y_j^{\bar{u}}\}_{j=1}^{d^{\bar{u}}}$, where $y_j^{\bar{u}} = x(\Delta t; x_j^{\bar{u}}, \bar{u})$ and the control inputs e_i , $i \in [m]$, are the unit vectors. In particular, we need no information about the state derivative but only require trajectory samples of the unknown nonlinear system (1) for a set of chosen control values.

The proposed learning approach crucially exploits that the Koopman operator acting on the defined lifting function Φ has a specific structure. In particular, note that Φ contains a constant observable $\phi_0 \equiv 1$, i.e., $\phi_0(x_{k+1}) = \phi_0(x_k) = 1$, and that $(\mathcal{K}_{\Delta t}^0)_{21} = 0$ due to $f(0) = 0$. Therefore, using (3), we obtain the (2×2) block-matrix representation

$$\mathcal{K}_{\Delta t}^u = \begin{bmatrix} 1 & 0 \\ (\mathcal{K}_{\Delta t}^u)_{21} & (\mathcal{K}_{\Delta t}^u)_{22} \end{bmatrix}, \quad (8a)$$

$$\mathcal{K}_{\Delta t}^0 = \begin{bmatrix} 1 & 0 \\ 0 & (\mathcal{K}_{\Delta t}^0)_{22} \end{bmatrix}, \quad \mathcal{K}_{\Delta t}^{e_i} = \begin{bmatrix} 1 & 0 \\ (\mathcal{K}_{\Delta t}^{e_i})_{21} & (\mathcal{K}_{\Delta t}^{e_i})_{22} \end{bmatrix}. \quad (8b)$$

Due to the structure of the Koopman operator in (8), we enforce the same structure for the data-driven surrogates in our proposed architecture, i.e., we consider

$$\mathcal{K}_{\Delta t, d}^0 = \begin{bmatrix} 1 & 0 \\ 0 & A \end{bmatrix}, \quad \mathcal{K}_{\Delta t, d}^{e_i} = \begin{bmatrix} 1 & 0 \\ B_{0,i} & \hat{B}_i \end{bmatrix}. \quad (9)$$

To learn the unknown matrices A , $B_{0,i}$, \hat{B}_i , we arrange the data \mathcal{D} in

$$X^{e_i} = [\Phi(x_1^{e_i}) \quad \cdots \quad \Phi(x_{d^{e_i}}^{e_i})], \quad (10a)$$

$$X^0 = \begin{bmatrix} \begin{bmatrix} \phi_1(x_1^0) \\ \vdots \\ \phi_N(x_1^0) \end{bmatrix} & \cdots & \begin{bmatrix} \phi_1(x_{d^0}^0) \\ \vdots \\ \phi_N(x_{d^0}^0) \end{bmatrix} \end{bmatrix}, \quad (10b)$$

$$Y^{\bar{u}} = \begin{bmatrix} \begin{bmatrix} \phi_1(y_1^{\bar{u}}) \\ \vdots \\ \phi_N(y_1^{\bar{u}}) \end{bmatrix} & \cdots & \begin{bmatrix} \phi_1(x_{d^{\bar{u}}}^{\bar{u}}) \\ \vdots \\ \phi_N(x_{d^{\bar{u}}}^{\bar{u}}) \end{bmatrix} \end{bmatrix}. \quad (10c)$$

The proposed learning architecture relies on solving the linear regression problems

$$A = \arg \min_{A \in \mathbb{R}^{N \times N}} \|Y^0 - AX^0\|_F, \quad (11a)$$

$$[B_{0,i} \quad \hat{B}_i] = \arg \min_{\substack{B_{0,i} \in \mathbb{R}^N, \\ \hat{B}_i \in \mathbb{R}^{N \times N}}} \|Y^{e_i} - [B_{0,i} \quad \hat{B}_i] X^{e_i}\|_F \quad (11b)$$

for $i \in [m]$, where $\|\cdot\|_F$ denotes the Frobenius norm. Based on the estimated matrices, we can construct a data-driven surrogate model for the discretization of the nonlinear dynamical system (1), i.e.,

$$\mathcal{K}_{\Delta t, d}^u = \mathcal{K}_{\Delta t, d}^0 + \sum_{i=1}^m u_i (\mathcal{K}_{\Delta t, d}^{e_i} - \mathcal{K}_{\Delta t, d}^0).$$

This model, however, is only an approximation of the true Koopman operator in (7), meaning that

$$\Phi(x_{k+1}) \approx \mathcal{K}_{\Delta t, d}^u \Phi(x_k). \quad (12)$$

The error is due to the different sources, including the bilinear approximation (3) as well as the above data-driven estimation. In the following main result, which forms the foundation of the proposed learning architecture, we provide a rigorous analysis of this error.

Theorem 3.1. *Suppose that Assumption 2.1 holds and the data samples \mathcal{D} are i.i.d. Then, for any probabilistic tolerance $\delta \in (0, 1)$, amount of data $d_0 \in \mathbb{N}$ and sampling rate $\Delta t > 0$, there are constants $c_x, c_u = \mathcal{O}(1/\sqrt{\delta d_0} + \Delta t^2)$ such that for all $d \geq d_0$, the learning error bound*

$$\|\mathcal{K}_{\Delta t}^u \Phi(x) - \mathcal{K}_{\Delta t, d}^u \Phi(x)\| \leq c_x \|\Phi(x) - \Phi(0)\| + c_u \|u\| \quad (13)$$

holds for all $x \in \mathbb{X}$ and $u \in \mathbb{U}$ with probability $1 - \delta$.

Algorithm 1 SafEDMD: Certified learning architecture tailored to data-driven control of nonlinear dynamical systems

Input: data $\mathcal{D} = \{x_j^{\bar{u}}, y_j^{\bar{u}}\}_{j=1}^d$ for $\bar{u} = 0, e_1, \dots, e_m$ with $y_j^{\bar{u}} = x(\Delta t; x_j^{\bar{u}}, \bar{u})$, observables Φ
 Arrange data in (10).

Solve (11).

Output: certified Koopman representation (12) with $\mathcal{K}_{\Delta t, d}^0, \mathcal{K}_{\Delta t, d}^{e_1}, \dots, \mathcal{K}_{\Delta t, d}^{e_m}$ defined in (9)

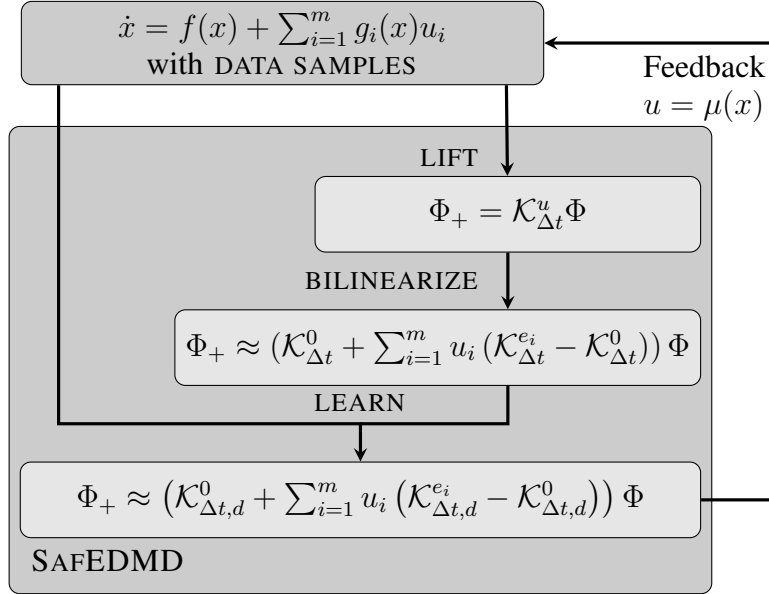


Fig. 2. Certified data-driven controller design for nonlinear dynamical systems. The overall scheme consists of two main steps: 1) learning a reliable surrogate model along with error bounds using SafEDMD; 2) designing a safe feedback controller $u = \mu(x)$ which robustly stabilizes the surrogate model. The approach yields certified safety guarantees due to the rigorous foundation based on SafEDMD, which learns a bilinear approximation of the (lifted) Koopman operator dynamics using data samples.

Proof (Sketch). We prove the result in two steps, where we first bound the error of the bilinear representation for the true Koopman operator $\mathcal{K}_{\Delta t}^u$ in (3) and then incorporate the estimation error from learning the bilinearized Koopman operator from data. The details are presented in Appendix A. \square

The error bound (13) of above Theorem 3.1 features two central ingredients crucial for design. The first aspect is that it is proportional in the sense that the right-hand side vanishes for $(x, u) = 0$. Such a proportional bound is, to the best of the authors' knowledge, so far not present in any learning scheme using the notably simple EDMD-framework and is decisive for controller design such that the underlying true system is reliably and safely operated by feedback control in a region containing the origin. The second point is that the proportionality constants c_x and c_u in (13) can be made arbitrarily small when choosing a sufficiently high amount of data points d_0 and a small enough sampling rate Δt . This is important for a successful controller design since the considered safety objective requires robustness against all possible learning errors satisfying the bound in (13).

The proposed learning architecture tailored to data-driven control of nonlinear dynamical systems based on the linear regression problems (11) and the error bound (13) is summarized in Algorithm 1.

4. CERTIFIED DATA-DRIVEN CONTROLLER DESIGN FOR NONLINEAR SYSTEMS

In this section, we use the certified learning architecture SafEDMD presented in Section 3 to design a safe controller for the sampled system (6). More precisely, our goal is to find a state-feedback controller $\mu : \mathbb{R}^n \rightarrow \mathbb{R}^m$ such that the setpoint is exponentially stable in closed loop using the control input $u_k = \mu(x_k)$, i.e., it is stable [31] and trajectories exponentially converge to the setpoint. Without loss of

generality, we assume that the setpoint is the origin $x = 0$. To find a suitable controller, we first proceed as in Algorithm 1 to obtain a data-driven surrogate model of the unknown nonlinear system based on sampled data. We then use this surrogate model along with the error bound in Theorem 3.1 in order to design a data-driven controller with a stability certificate. The overall control scheme is illustrated in Fig. 2

To obtain rigorous safety guarantees, our proposed controller ensures that the system trajectories evolve in a predetermined set $\Delta_\Phi = \{\psi \in \mathbb{R}^N \mid (14) \text{ holds}\}$ with

$$\begin{bmatrix} \psi \\ 1 \end{bmatrix}^\top \begin{bmatrix} Q_z & S_z \\ S_z^\top & R_z \end{bmatrix} \begin{bmatrix} \psi \\ 1 \end{bmatrix} \geq 0 \quad (14)$$

for fixed matrices $Q_z \in \mathbb{R}^{N \times N}$, $S_z \in \mathbb{R}^N$, $R_z \in \mathbb{R}$ with $Q_z \prec 0$ and $R_z > 0$ for which the inverse

$$\begin{bmatrix} \tilde{Q}_z & \tilde{S}_z \\ \tilde{S}_z & \tilde{R}_z \end{bmatrix} := \begin{bmatrix} Q_z & S_z \\ S_z^\top & R_z \end{bmatrix}^{-1}$$

exists. In particular, we enforce $\hat{\Phi}(x) \in \Delta_\Phi$ for all times. The parametrization of Δ_Φ includes, e.g., a simple norm bound $\|\hat{\Phi}(x)\|^2 \leq c$ for all x by choosing $Q_z = -I$, $S_z = 0$, and $R_z = c$. More sophisticated parametrizations are also possible by including prior knowledge of the system or using heuristics (compare [18, Sec. V]). The set Δ_Φ needs to be defined by the user before applying the following controller design procedure. Ideally, one chooses Δ_Φ preferably large since it determines an outer bound on the safe operating region in which the proposed controller reliably controls the system. However, there is a trade-off since too large choices of Δ_Φ may lead to an infeasible controller design. In Section 5, we discuss practical possibilities for choosing Δ_Φ using numerical examples.

The following theorem establishes a controller design method guaranteeing safe operation by exponential stability of the *sampled* nonlinear system (6) by solving an LMI feasibility problem.

Theorem 4.1. *Let Assumption 2.1 hold and the data points \mathcal{D} be sampled i.i.d. from \mathbb{X} . Suppose a data-driven surrogate model of the unknown nonlinear system (1) as learned using the certified learning architecture defined in Theorem 3.1 with given probabilistic tolerance $\delta \in (0, 1)$ and constants $c_x > 0$ and $c_u > 0$.*

If there exist a matrix $0 \prec P = P^\top \in \mathbb{R}^{N \times N}$, matrices $L \in \mathbb{R}^{m \times N}$, $L_w \in \mathbb{R}^{m \times Nm}$, a matrix $0 \prec \Lambda = \Lambda^\top \in \mathbb{R}^{m \times m}$, and scalars $\nu > 0$, $\tau > 0$ such that

$$\begin{bmatrix} P - \tau I_N & -\tilde{B}(\Lambda \otimes \tilde{S}_z) - B_0 L_w (I_m \otimes \tilde{S}_z) & 0 & AP + B_0 L & \tilde{B}(\Lambda \otimes I_N) + B_0 L_w \\ \star & (\Lambda \otimes \tilde{R}_z) - L_w (I_m \otimes \tilde{S}_z) - (I_m \otimes \tilde{S}_z^\top) L_w^\top & -(I_m \otimes \tilde{S}_z^\top) \begin{bmatrix} 0 \\ L_w \end{bmatrix} & L & L_w \\ \star & \star & 0.5\tau \begin{bmatrix} c_x^{-2} I_N & 0 \\ 0 & c_u^{-2} I_m \end{bmatrix} & \begin{bmatrix} P \\ L \\ P \end{bmatrix} & - \begin{bmatrix} 0 \\ L_w \\ 0 \end{bmatrix} \\ \star & \star & \star & \star & 0 \\ \star & \star & \star & \star & -(\Lambda \otimes \tilde{Q}_z^{-1}) \end{bmatrix} \succ 0 \quad (15)$$

and

$$\begin{bmatrix} \nu \tilde{R}_z - 1 & -\nu \tilde{S}_z^\top \\ -\nu \tilde{S}_z & \nu \tilde{Q}_z + P \end{bmatrix} \preceq 0 \quad (16)$$

hold, then there exists an amount of data $d_0 \in \mathbb{N}$ such that for all $d \geq d_0$ the controller³

$$\mu(x) = (I - L_w(\Lambda^{-1} \otimes \hat{\Phi}(x)))^{-1} L P^{-1} \hat{\Phi}(x) \quad (17)$$

ensures safe operation by exponential stability of the sampled nonlinear system (6) for all initial conditions inside the safe operating region $\hat{x} \in \mathcal{X}_{\text{SOR}} := \{x \in \mathbb{R}^n \mid \hat{\Phi}(x)^\top P^{-1} \hat{\Phi}(x) \leq 1\}$ with probability $1 - \delta$.

³By \otimes we refer to the Kronecker product.

Proof (Sketch). The result can be shown in two steps. First, we need to show that all $x \in \mathcal{X}_{\text{SOR}}$ satisfy $\hat{\Phi}(x) \in \Delta_{\Phi}$. Then, we conclude positive invariance of \mathcal{X}_{SOR} together with exponential stability of the sampled closed-loop system (6) for all $\hat{x} \in \mathcal{X}_{\text{SOR}}$. This directly ensures safe operation under the obtained feedback via the used certified learning architecture of Theorem 3.1. The proof is detailed in Appendix B. \square

The proposed controller design in Theorem 4.1 is purely based on data samples of the state trajectory and does not rely on model knowledge. In particular, we use the certified learning scheme SafEDMD of Theorem 3.1 to obtain a reliable data-driven system parametrization. We emphasize that the controller design is framed as a semi-definite program using linear matrix inequalities which can be efficiently solved (cf. [32]). The robust controller uses the learning error bounds in (13) to ensure safe operation of the resulting controller when applied to the unknown nonlinear system. Here, we can directly relate a given desired accuracy and certainty about the closed-loop guarantees as well as the input dimension m to the necessary amount of data d_0 and the sampling period Δt .

We note that the controller parametrization (17) contains the control law $\mu(x) = K\hat{\Phi}(x)$, which is linear in the lifted state, as a special case for $L_w = 0$ and $K = LP^{-1}$. However, our proposed nonlinear controller parametrization (17) achieves larger regions of safe operation \mathcal{X}_{SOR} for which we can guarantee reliable behavior in closed loop.

On a technical level, the controller design approach in Theorem 4.1 follows similar ideas as in [18]. The key difference of Theorem 4.1 to this existing work is that the latter designs a data-driven controller based on an estimate of the Koopman *generator*, i.e., it involves learning a continuous-time model and designing a controller, which continuously changes the respective control values. The key disadvantage of the proposed scheme in [18] is that derivative measurements are required, which limits its practical use, especially in the presence of noisy data. Instead, here, Theorem 4.1 relies on a discrete-time controller design for the sampled nonlinear system with sample-and-hold implementation of the control signal (6) (compare [33], [34]). The main contribution of the introduced controller design is the tight connection to the SafEDMD learning architecture and, hence, it leads to reliable and certified guarantees for the true nonlinear system purely based on (non-derivative) data.

Corollary 4.2. *Let the assumptions of Theorem 4.1 hold and suppose additionally that the vector field $f_c : \mathbb{R}^n \times \mathbb{R}^m \rightarrow \mathbb{R}^n$ with $f_c(x, u) = f(x) + g(x)u$ corresponding to the nonlinear system (1) is continuous and locally Lipschitz in its first argument around the origin.*

If there exist a matrix $0 \prec P = P^\top \in \mathbb{R}^{N \times N}$, matrices $L \in \mathbb{R}^{m \times N}$, $L_w \in \mathbb{R}^{m \times Nm}$, a matrix $0 \prec \Lambda = \Lambda^\top \in \mathbb{R}^{m \times m}$, and scalars $\nu > 0$, $\tau > 0$ such that (15) and (16) hold, then there exists an amount of data $d_0 \in \mathbb{N}$ such that for all $d \geq d_0$ the controller

$$\mu_s(x(t)) = \mu(x(k\Delta t)), \quad t \in [k\Delta t, (k+1)\Delta t), \quad k \geq 0 \quad (18)$$

ensures safe operation by exponential stability of the continuous-time nonlinear system (1) for all initial conditions $\hat{x} \in \mathcal{X}_{\text{SOR}} := \{x \in \mathbb{R}^n \mid \hat{\Phi}(x)^\top P^{-1} \hat{\Phi}(x) \leq 1\}$ with probability $1 - \delta$.

Proof. This result can be proven building on [35, Thm. 2.27], which is elaborated in Appendix C. \square

This corollary uses the stability certificates in Theorem 4.1, which are obtained for the sampled system (6), to infer the certificates also for the *true* continuous-time nonlinear system (1) using sampled feedback. Hence, the obtained closed-loop guarantees based on the introduced certified learning architecture hold for both sampled and continuous-time nonlinear systems.

5. NUMERICAL EXPERIMENTS

To evaluate the practicality of the proposed SafEDMD architecture, we perform a numerical study and compare our results to state-of-the-art Koopman-based lifting and control. All our simulations are conducted in Matlab using the toolbox [36] with the semi-definite programming solver MOSEK [37].

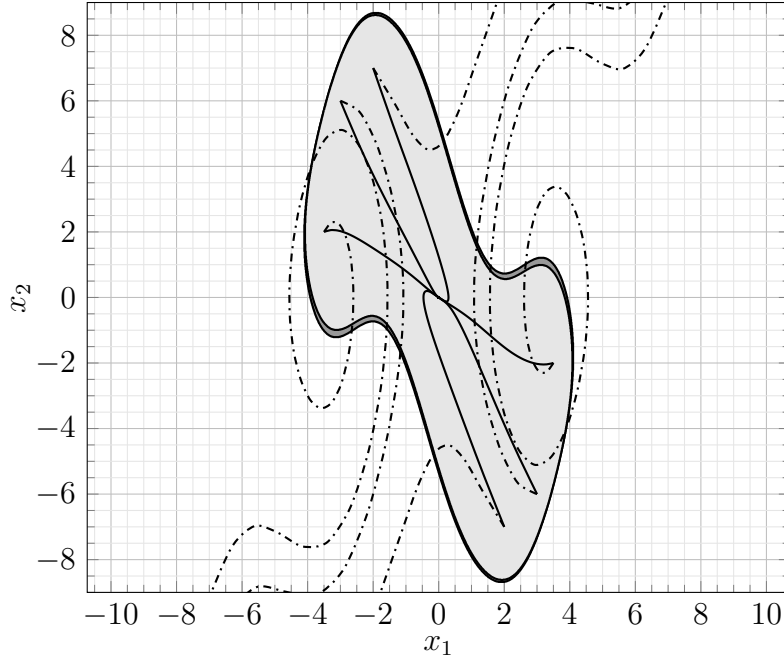


Fig. 3. Region containing all x with $\hat{\Phi}(x) \in \Delta_{\Phi}$ (\bullet), safe operating region \mathcal{X}_{SOR} (\circ), and closed-loop trajectories for the controller μ (—) corresponding to the experiment in Section 5.1, and, for comparison, closed-loop trajectories for the controller μ_{LQR} (---).

5.1. Nonlinear inverted pendulum

The inverted pendulum is a classical example for dynamical systems, which is often used as a benchmark in nonlinear data-driven control, cf. [38]–[42]. This dynamical system can be modeled by

$$\begin{aligned}\dot{x}_1(t) &= x_2(t), \\ \dot{x}_2(t) &= \frac{g}{l} \sin(x_1(t)) - \frac{b}{ml^2} x_2(t) + \frac{1}{ml^2} u(t)\end{aligned}$$

with mass m , length l , rotational friction coefficient b , and gravitational constant $g = 9.81$ m/s.

Our experiments are performed with $m = 1$, $l = 1$, and $b = 0.01$. Further, we define the sets $\mathbb{X} = [-2, 10]^2$ and $\mathbb{U} = [-10, 10]$ whereof we uniformly sample $d = 6000$ data points with sampling period $\Delta t = 0.01$ s. We use the observable functions $\hat{\Phi}(x) = [x_1 \ x_2 \ \sin(x_1)]^\top$, where the sine function is inferred by some prior knowledge on the underlying nonlinear system. We use the proposed certified learning architecture SafEDMD in Algorithm 1, where Theorem 3.1 yields a data-driven surrogate model as in (12) with certified learning error bounds with probabilistic tolerance $\delta = 0.05$ and $c_x = c_u = 3 \times 10^{-4}$ by linear regression.

To illustrate the obtained certificates, we apply the robust controller design in Section 4 guaranteeing safe operation and closed-loop exponential stability of the nonlinear system via Theorem 4.1. In order to apply the proposed design scheme, we predefine the outer bound Δ_{Φ} on the safe operating region following the approach in [18, Procedure 7]. In particular, we first solve (15) for $\tilde{Q}_z = -I$, $\tilde{S}_z = 0$, and arbitrary $\tilde{R}_z > 0$ without considering the second liner matrix inequality (16). This leads to a matrix P which relates the measured data and the chosen observables to infer a likely behavior of the closed-loop system, such that the safe operating region is maximized according to the underlying system dynamics. Then, we incorporate this information in the actual controller design by defining Δ_{Φ} via $Q_z = -\frac{P^{-1}}{\|P^{-1}\|_2}$, $S_z = 0$, and $R_z > 0$. Designing the nonlinear state-feedback controller (17) via Theorem 4.1 leads to the operation region depicted in Fig. 3, for which we can safely and reliably apply the control law μ to the true nonlinear system. The closed-loop trajectories of the nonlinear system highlight that the system is indeed stabilized by our controller inside of the obtained region.

Next, we compare the learned surrogate model using SafEDMD to the state-of-the-art Koopman learning in the literature. In particular, we compare with the learned system model using EDMDC and a linear representation in state and control in the surrogate model, see, e.g., [10], [28]. To this end, we define the lifted Koopman model

$$\hat{\Phi}_+ \approx \check{A}\hat{\Phi} + \check{B}u \quad (19)$$

via the linear regression

$$\min_{\check{A}, \check{B}} \left\| \begin{bmatrix} \hat{\Phi}(X_+^0) & \hat{\Phi}(X_+^{e1}) & \dots & \hat{\Phi}(X_+^{em}) \end{bmatrix} - [\check{A} \ \check{B}] \begin{bmatrix} \hat{\Phi}(X^0) & \hat{\Phi}(X^{e1}) & \dots & \hat{\Phi}(X^{em}) \end{bmatrix} \right\|. \quad (20)$$

For the comparison, we use a discrete-time linear-quadratic regulation (LQR) controller $\mu_{\text{LQR}} = \check{K}\hat{\Phi}(x)$, where \check{K} is defined by

$$\check{K} = (R + \check{B}^\top \check{P} \check{B})^{-1} \check{B}^\top \check{P} \check{A}$$

with \check{P} denoting the solution to the discrete-time algebraic Riccati equation

$$\check{P} = \check{A}^\top \check{P} \check{A} - \check{A}^\top \check{P} \check{B} (R + \check{B}^\top \check{P} \check{B})^{-1} \check{B}^\top \check{P} \check{A} + Q$$

and $Q = R = I$ for simplicity. Fig. 3 illustrates that the obtained model in (19) has no certificates of its learning quality or error, and, thus, the LQR controller is not able to stabilize the underlying nonlinear system. On the other hand, the proposed certified learning architecture SafEDMD with a bilinear lifted model and guaranteed learning error bounds leads to a stabilizing controller for the *unknown* nonlinear system (1) using the same data samples

5.2. Nonlinear system with Koopman invariant observables

Next, we consider the nonlinear system

$$\begin{aligned} \dot{x}_1(t) &= \rho x_1(t), \\ \dot{x}_2(t) &= \lambda(x_2(t) - x_1(t)^2) + u(t) \end{aligned}$$

with $\rho, \lambda \in \mathbb{R}$. This example system is a common benchmark example since it permits the definition of an invariant dictionary [28]. More precisely, the observable function

$$\hat{\Phi}(x) = \begin{bmatrix} x_1 & x_2 & x_2 - \frac{\lambda}{\lambda - 2\rho} x_1^2 \end{bmatrix}^\top$$

leads to *exact* finite-dimensional lifted continuous-time dynamics

$$\frac{d}{dt} \hat{\Phi}(x(t)) = \begin{bmatrix} \rho & 0 & 0 \\ 0 & 2\rho & \lambda - 2\rho \\ 0 & 0 & \lambda \end{bmatrix} \hat{\Phi}(x(t)) + \begin{bmatrix} 0 \\ 1 \\ 1 \end{bmatrix} u(t). \quad (21)$$

Here, even though $\hat{\Phi}$ is Koopman-invariant and (21) is exact, the formulation is exposed to a major drawback: The lifted dynamics are time-continuous, i.e., information on the state derivative is necessary in order to learn the exact continuous time dynamics from data. In particular, the derivative data either needs to be measured directly or estimated based on sample data. This, however, introduces errors (in particular in the presence of noise) and, thus, prevents safe and reliable learning of the underlying true system. Contrary, the proposed SafEDMD learning provides a reliable surrogate model that is purely based on sample data of the state x and, particularly, without the need for derivative data.

We consider the parameters $\rho = -2$ and $\lambda = 1$ and sample $d = 100$ data points uniformly from the sets $\mathbb{X} = [-1, 1]^2$ and $\mathbb{U} = [-1, 1]$ with sampling rate $\Delta t = 0.01$ s. Then, we learn a certified data-driven surrogate model via SafEDMD based on the generated data set. For a probabilistic tolerance $\delta = 0.05$ and constants $c_x = c_x = 5 \times 10^{-3}$ for the learning error bound (13), we apply the controller design in Theorem 4.1 with Δ_Φ defined by $Q_z = -I$, $S_z = 0$, and $R_z = 500$. The obtained controller is guaranteed to ensure safe operation in the region \mathcal{X}_{SOR} shown in Fig. 4. Here, \mathcal{X}_{SOR} contains all x with $\hat{\Phi}(x) \in \Delta_\Phi$

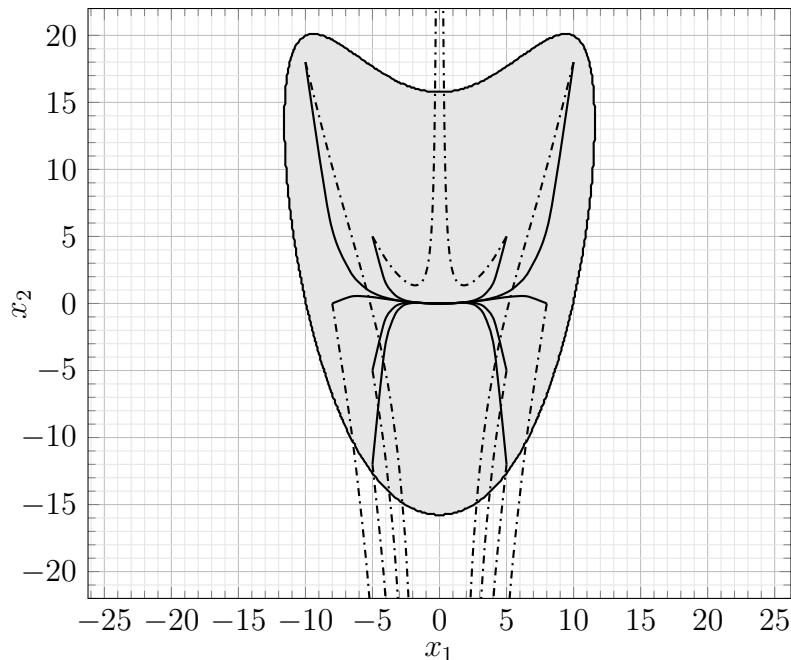


Fig. 4. Safe operating region \mathcal{X}_{SOR} (\odot) and closed-loop trajectories for the controller μ (—) corresponding to the experiment in Section 5.2, and, for comparison, closed-loop trajectories for the controller μ_{LQR} (- - -).

and, thus, adds no additional conservatism to the robust controller design. We emphasize again that the closed loop under our proposed certified control law μ operates reliably in the sense that it exponentially converges to the origin. On the contrary, the established approach of designing an LQR controller μ_{LQR} based on the linear lifted system (19) learned via linear EDMD (20) leads to an unstable and, hence, unsafe behavior of the nonlinear system.

6. CONCLUSION

In conclusion, this paper introduced SafEDMD, a certified learning architecture tailored to data-driven control of nonlinear dynamical systems. Leveraging the analytical foundation of the Koopman operator, we showed that SafEDMD enables a rigorous and certified derivation of error bounds crucial for robust controller design. Unlike existing methods, the proposed architecture handles the Koopman operator directly via sampled data, eliminating the need for hard-to-obtain time-derivative data. SafEDMD offers a promising direction for the certified control of unknown nonlinear systems, demonstrating its superiority in scenarios where existing methods fail. This research not only tailors the capabilities of bilinear EDMD for control tasks but also establishes a new paradigm in the field of learning and control of data-driven surrogate models with rigorous stability certificates, addressing a critical aspect in safety-critical applications.

Interesting future work includes the integration of deep NNs as the observable function to exploit the superior robustness and scalability of EDMD-based approaches compared to state-of-the-art reinforcement learning methods (compare [43]).

REFERENCES

- [1] M. Williams, I. Kevrekidis, and C. Rowley, “A data-driven approximation of the Koopman operator: Extending dynamic mode decomposition,” *Journal of Nonlinear Science*, vol. 25, no. 6, pp. 1307–1346, 08 2015.
- [2] O. Azencot, N. B. Erichson, V. Lin, and M. Mahoney, “Forecasting sequential data using consistent Koopman autoencoders,” in *International Conference on Machine Learning*. PMLR, 2020, pp. 475–485.
- [3] T. Golany, K. Radinsky, D. Freedman, and S. Minha, “12-lead eeg reconstruction via Koopman operators,” in *International Conference on Machine Learning*. PMLR, 2021, pp. 3745–3754.

- [4] S. Klus, F. Nüske, and S. Peitz, “Koopman analysis of quantum systems,” *Journal of Physics A: Mathematical and Theoretical*, vol. 55, no. 31, p. 314002, 2022.
- [5] R. Strässer, S. Schlor, and F. Allgöwer, “Decrypting nonlinearity: Koopman interpretation and analysis of cryptosystems,” *arXiv:2311.12714*, 2023.
- [6] I. Mezić, “Analysis of fluid flows via spectral properties of the Koopman operator,” *Annual review of fluid mechanics*, vol. 45, pp. 357–378, 2013.
- [7] V. Kostic, P. Novelli, A. Maurer, C. Ciliberto, L. Rosasco, and M. Pontil, “Learning dynamical systems via Koopman operator regression in reproducing kernel Hilbert spaces,” *Advances in Neural Information Processing Systems*, vol. 35, pp. 4017–4031, 2022.
- [8] F. Philipp, M. Schaller, K. Worthmann, S. Peitz, and F. Nüske, “Error bounds for kernel-based approximations of the Koopman operator,” *arXiv:2301.08637*, 2023.
- [9] C. Folkestad, Y. Chen, A. D. Ames, and J. W. Burdick, “Data-driven safety-critical control: Synthesizing control barrier functions with Koopman operators,” *IEEE Control Systems Letters*, vol. 5, no. 6, pp. 2012–2017, 2020.
- [10] M. Korda and I. Mezić, “Linear predictors for nonlinear dynamical systems: Koopman operator meets model predictive control,” *Automatica*, vol. 93, pp. 149–160, 2018.
- [11] J. L. Proctor, S. L. Brunton, and J. N. Kutz, “Generalizing Koopman theory to allow for inputs and control,” *SIAM Journal on Applied Dynamical Systems*, vol. 17, no. 1, pp. 909–930, 2018.
- [12] M. O. Williams, M. S. Hemati, S. T. Dawson, I. G. Kevrekidis, and C. W. Rowley, “Extending data-driven Koopman analysis to actuated systems,” *IFAC-PapersOnLine*, vol. 49, no. 18, pp. 704–709, 2016.
- [13] A. Surana, “Koopman operator based observer synthesis for control-affine nonlinear systems,” in *Proc. 55th IEEE Conference on Decision and Control (CDC)*, 2016, pp. 6492–6499.
- [14] P. Bevanda, S. Sosnowski, and S. Hirche, “Koopman operator dynamical models: Learning, analysis and control,” *Annual Reviews in Control*, vol. 52, pp. 197–212, 2021.
- [15] M. Korda and I. Mezić, “On convergence of extended dynamic mode decomposition to the Koopman operator,” *Journal of Nonlinear Science*, vol. 28, no. 2, pp. 687–710, 2018.
- [16] F. Nüske, S. Peitz, F. Philipp, M. Schaller, and K. Worthmann, “Finite-data error bounds for Koopman-based prediction and control,” *Journal of Nonlinear Science*, vol. 33, no. 1, p. 14, 2023.
- [17] L. Bold, L. Grüne, M. Schaller, and K. Worthmann, “Practical asymptotic stability of data-driven model predictive control using extended DMD,” *arXiv:2308.00296*, 2023.
- [18] R. Strässer, M. Schaller, K. Worthmann, J. Berberich, and F. Allgöwer, “Koopman-based feedback design with stability guarantees,” *arXiv:2312.01441*, 2023.
- [19] B. O. Koopman, “Hamiltonian systems and transformation in Hilbert space,” *Proc. of the National Academy of Sciences of the United States of America*, vol. 17, no. 5, p. 315, 1931.
- [20] P. van Goor, R. Mahony, M. Schaller, and K. Worthmann, “Reprojection methods for Koopman-based modelling and prediction,” in *Proc. 62nd IEEE Conference on Decision and Control (CDC)*, 2023, pp. 315–321.
- [21] S. Peitz, S. E. Otto, and C. W. Rowley, “Data-driven model predictive control using interpolated Koopman generators,” *SIAM Journal on Applied Dynamical Systems*, vol. 19, no. 3, pp. 2162–2193, 2020.
- [22] F. Philipp, M. Schaller, K. Worthmann, S. Peitz, and F. Nüske, “Error analysis of kernel EDMD for prediction and control in the Koopman framework,” *arXiv:2312.10460*, 2023.
- [23] Q. Li, F. Dietrich, E. M. Bollt, and I. G. Kevrekidis, “Extended dynamic mode decomposition with dictionary learning: A data-driven adaptive spectral decomposition of the Koopman operator,” *Chaos: An Interdisciplinary Journal of Nonlinear Science*, vol. 27, no. 10, 2017.
- [24] L. Shi and K. Karydis, “Ac-dmd: Analytical construction for dictionaries of lifting functions in Koopman operator-based nonlinear robotic systems,” *IEEE Robotics and Automation Letters*, vol. 7, no. 2, pp. 906–913, 2021.
- [25] E. Yeung, S. Kundu, and N. Hodas, “Learning deep neural network representations for Koopman operators of nonlinear dynamical systems,” in *IEEE American Control Conference. ACC*, 2019, pp. 4832–4839.
- [26] P. Pauli, A. Koch, J. Berberich, P. Kohler, and F. Allgöwer, “Training robust neural networks using Lipschitz bounds,” *IEEE Control Systems Letters*, vol. 6, pp. 121–126, 2021.
- [27] D. Goswami and D. A. Paley, “Bilinearization, reachability, and optimal control of control-affine nonlinear systems: A Koopman spectral approach,” *IEEE Transactions on Automatic Control*, vol. 67, no. 6, pp. 2715–2728, 2021.
- [28] S. L. Brunton, B. W. Brunton, J. L. Proctor, and J. N. Kutz, “Koopman invariant subspaces and finite linear representations of nonlinear dynamical systems for control,” *PloS one*, vol. 11, no. 2, pp. 1–19, 2016.
- [29] M. Korda and I. Mezić, “Optimal construction of Koopman eigenfunctions for prediction and control,” *IEEE Transactions on Automatic Control*, vol. 65, no. 12, pp. 5114–5129, 2020.
- [30] M. Schaller, K. Worthmann, F. Philipp, S. Peitz, and F. Nüske, “Towards reliable data-based optimal and predictive control using extended DMD,” *IFAC-PapersOnLine*, vol. 56, no. 1, pp. 169–174, 2023.
- [31] H. K. Khalil, *Nonlinear systems*, 3rd ed. Upper Saddle River, NJ: Prentice-Hall, 2002.
- [32] L. Vandenberghe and S. Boyd, “Semidefinite programming,” *SIAM review*, vol. 38, no. 1, pp. 49–95, 1996.
- [33] R. Strässer, J. Berberich, and F. Allgöwer, “Robust data-driven control for nonlinear systems using the Koopman operator,” *IFAC-PapersOnLine*, vol. 56, no. 2, pp. 2257–2262, 2023.
- [34] R. Strässer, J. Berberich, and F. Allgöwer, “Control of bilinear systems using gain-scheduling: Stability and performance guarantees,” in *Proc. 62nd IEEE Conference on Decision and Control (CDC)*, 2023, pp. 4674–4681.
- [35] L. Grüne and J. Pannek, *Nonlinear model predictive control*. Springer, 2017.
- [36] J. Löfberg, “YALMIP: A toolbox for modeling and optimization in MATLAB,” in *Proc. IEEE International Conference on Robotics and Automation*, 2004, pp. 284–289.
- [37] M. ApS, *The MOSEK optimization toolbox for MATLAB manual. Version 9.3.21*, 2022.

- [38] T. Bertalan, F. Dietrich, I. Mezić, and I. G. Kevrekidis, “On learning Hamiltonian systems from data,” *Chaos: An Interdisciplinary Journal of Nonlinear Science*, vol. 29, no. 12, 2019.
- [39] R. Strässer, J. Berberich, and F. Allgöwer, “Data-driven control of nonlinear systems: Beyond polynomial dynamics,” in *Proc. 60th IEEE Conference on Decision and Control (CDC)*, 2021, pp. 4344–4351.
- [40] C. Verhoek, H. S. Abbas, and R. Tóth, “Direct data-driven LPV control of nonlinear systems: An experimental result,” *IFAC-PapersOnLine*, vol. 56, no. 2, pp. 2263–2268, 2023.
- [41] M. Tiwari, G. Nehma, and B. Lusch, “Computationally efficient data-driven discovery and linear representation of nonlinear systems for control,” *IEEE Control Systems Letters*, vol. 7, pp. 3373–3378, 2023.
- [42] T. Martin, T. B. Schön, and F. Allgöwer, “Guarantees for data-driven control of nonlinear systems using semidefinite programming: A survey,” *Annual Reviews in Control*, p. 100911, 2023.
- [43] M. Han, J. Euler-Rolle, and R. K. Katzschmann, “DeSKO: Stability-assured robust control with a deep stochastic Koopman operator,” in *International Conference on Learning Representations*. ICLR, 2022.
- [44] C. W. Scherer and S. Weiland, “Linear matrix inequalities in control,” *Lecture Notes, Dutch Institute for Systems and Control, Delft, The Netherlands*, vol. 3, no. 2, 2000.
- [45] S. P. Boyd and L. Vandenberghe, *Convex Optimization*. Cambridge University Press, 2004.

APPENDIX

A. Proof of Theorem 3.1

In this section, we prove Theorem 3.1, which introduces SafEDMD: A novel certified learning architecture for data-driven control of nonlinear dynamical systems. To this end, we first introduce a finite-dimensional bilinear representation for the Koopman operator in Lemma A.1 before defining a data-driven surrogate model for the bilinear representation in Lemma A.3. Then, Theorem 3.1 results as a direct consequence of the preliminary lemmas.

1) *Bilinear representation for the Koopman operator*: The proposed certified learning architecture relies on a bilinear representation of the Koopman operator $\mathcal{K}_{\Delta t}^u$. For the setting in this paper and for a fixed control value $u \in \mathbb{U}$, $(\mathcal{K}_t^u)_{t \geq 0}$ is a strongly-continuous semigroup of bounded linear operators, i.e., we can define its infinitesimal generator \mathcal{L}^u via

$$\mathcal{L}^u \varphi := \lim_{t \searrow 0} \frac{\mathcal{K}_t^u \varphi - \varphi}{t} \quad \forall \varphi \in D(\mathcal{L}^u),$$

where the domain $D(\mathcal{L}^u)$ consists of all L^2 -functions for which the above limit exists. By definition of this generator, the propagated observable satisfies $\dot{\varphi}(x) = \mathcal{L}^u \varphi(x)$. A key structural property of the Koopman generator, also called Liouville operator, is that control affinity is preserved [12], [13], i.e., for $u \in \mathbb{R}^m$ we have

$$\mathcal{L}^u = \mathcal{L}^0 + \sum_{i=1}^m u_i (\mathcal{L}^{e_i} - \mathcal{L}^0), \quad (22)$$

where \mathcal{L}^0 and \mathcal{L}^{e_i} , $i \in [m]$, are the generators of the Koopman semigroups corresponding to the constant control functions $u \equiv 0$ and $u \equiv e_i$ with the unit vector e_i , $i \in [m]$, respectively. Hence, the Koopman generator acting on the vector-valued observable function Φ in (4) has a specific structure due to the included constant observable $\phi_0 \equiv 1$. In particular, we obtain

$$\mathcal{L}^u = \begin{bmatrix} 0 & 0 \\ \mathcal{L}_{21}^u & \mathcal{L}_{22}^u \end{bmatrix} \quad \text{using the identity (22) with } \mathcal{L}^0 = \begin{bmatrix} 0 & 0 \\ 0 & \mathcal{L}_{22}^0 \end{bmatrix} \quad \text{and } \mathcal{L}^{e_i} = \begin{bmatrix} 0 & 0 \\ \mathcal{L}_{21}^{e_i} & \mathcal{L}_{22}^{e_i} \end{bmatrix}, i \in [m]. \quad (23)$$

The structure of the matrices in (23) corresponds to the structure of the Koopman operator (8) in the proposed learning architecture. We stress that in this work, the Koopman generator is only used in the proofs. In particular, our learning scheme directly approximates the Koopman operator by means of trajectory samples. This avoids the use of (typically extremely-noisy) derivative data necessary to approximate the Koopman generator in view of $\mathcal{L}\Phi(x) = \langle \nabla \Phi(x), \dot{x}(t) \rangle = \langle \nabla \Phi(x), f(x(t)) + \sum_{i=1}^m g_i(x(t))u_i(t) \rangle$. In conclusion, this makes our learning scheme data-efficient and robust in comparison to competing methods, for which similar error estimates exist [17], [18] and whose derivations have inspired the following lemma and its proof.

In the following, we leverage the control affine structure (22) of the generator \mathcal{L}^u to study the Koopman operator given by $\mathcal{K}_{\Delta t}^u = \exp(\Delta t \mathcal{L}^u)$. To this end, we recall (3) and define

$$\mathcal{K}_{\Delta t}^u = \mathcal{K}_{\Delta t}^0 + \sum_{i=1}^m u_i (\mathcal{K}_{\Delta t}^{e_i} - \mathcal{K}_{\Delta t}^0) + h(\Delta t)$$

with

$$h(\Delta t) := \mathcal{K}_{\Delta t}^u - \left[\mathcal{K}_{\Delta t}^0 + \sum_{i=1}^m u_i (\mathcal{K}_{\Delta t}^{e_i} - \mathcal{K}_{\Delta t}^0) \right]. \quad (24)$$

Further, we define $\xi(x, u) := h(\Delta t)\Phi(x)$ to obtain

$$\Phi(x_{k+1}) = \mathcal{K}_{\Delta t}^u \Phi(x_k) = \mathcal{K}_{\Delta t}^0 \Phi(x_k) + \sum_{i=1}^m u_{k,i} (\mathcal{K}_{\Delta t}^{e_i} - \mathcal{K}_{\Delta t}^0) \Phi(x_k) + \xi(x_k, u_k).$$

The following lemma formulates a proportional bound on the approximation error ξ of the bilinear representation of the Koopman operator.

Lemma A.1. *Suppose that Assumption 2.1 holds. Then, the approximation error ξ due to the bilinear representation of the Koopman operator $\mathcal{K}_{\Delta t}^u$ satisfies the proportional bound*

$$\|\xi(x, u)\| \leq \Delta t^2 (c_1 \|\Phi(x) - \Phi(0)\| + \sqrt{m} c_2 \|u\|), \quad (25)$$

where $c_1, c_2 \in \mathbb{R}_+$ are defined in (28) and (30).

Proof. Recall the definition of $\xi(x, u) = h(\Delta t)\Phi(x)$ with $h(\Delta t)$ defined in (24). Then, we bound the norm of $\xi(x, u)$ by

$$\begin{aligned} \|\xi(x, u)\| &= \|h(\Delta t)(\Phi(x) - \Phi(0) + \Phi(0))\| \leq \|h(\Delta t)(\Phi(x) - \Phi(0))\| + \|h(\Delta t)\Phi(0)\| \\ &\leq \|h(\Delta t)\| \|\Phi(x) - \Phi(0)\| + \|h(\Delta t)\Phi(0)\|. \end{aligned} \quad (26)$$

To estimate the first term in (26), we substitute $\mathcal{K}_{\Delta t}^u = e^{\Delta t \mathcal{L}^u}$, $\mathcal{K}_{\Delta t}^0 = e^{\Delta t \mathcal{L}^0}$, and $\mathcal{K}_{\Delta t}^{e_i} = e^{\Delta t \mathcal{L}^{e_i}}$, $i \in [m]$, to obtain

$$h(\Delta t) = e^{\Delta t (\mathcal{L}^0 + \sum_{i=1}^m u_i (\mathcal{L}^{e_i} - \mathcal{L}^0))} - \left(e^{\Delta t \mathcal{L}^0} + \sum_{i=1}^m u_i (e^{\Delta t \mathcal{L}^{e_i}} - e^{\Delta t \mathcal{L}^0}) \right). \quad (27)$$

Then, the Taylor series expansion for $h(\Delta t)$ at $\Delta t = 0$ yields

$$\begin{aligned} h(\Delta t) &= h(0) + \Delta t \frac{\partial h}{\partial \Delta t}(0) + \frac{\Delta t^2}{2} \frac{\partial^2 h}{\partial \Delta t^2}(\tau) \\ &= 0 + \Delta t \underbrace{\left[\left(\mathcal{L}^0 + \sum_{i=1}^m u_i (\mathcal{L}^{e_i} - \mathcal{L}^0) \right) - \left(\mathcal{L}^0 + \sum_{i=1}^m u_i (\mathcal{L}^{e_i} - \mathcal{L}^0) \right) \right]}_{=0} \\ &\quad + \frac{\Delta t^2}{2} \left[e^{\tau (\mathcal{L}^0 + \sum_{i=1}^m u_i (\mathcal{L}^{e_i} - \mathcal{L}^0))} \left(\mathcal{L}^0 + \sum_{i=1}^m u_i (\mathcal{L}^{e_i} - \mathcal{L}^0) \right)^2 \right. \\ &\quad \left. - \left(e^{\tau \mathcal{L}^0} (\mathcal{L}^0)^2 + \sum_{i=1}^m u_i (e^{\tau \mathcal{L}^{e_i}} (\mathcal{L}^{e_i})^2 - e^{\tau \mathcal{L}^0} (\mathcal{L}^0)^2) \right) \right] \end{aligned}$$

for some $\tau \in [0, \Delta t]$. Hence, we can derive the following estimate using the triangle inequality

$$\begin{aligned}
& \frac{2\|h(\Delta t)\|}{\Delta t^2} \\
& \leq \left\| e^{\tau(\mathcal{L}^0 + \sum_{i=1}^m u_i(\mathcal{L}^{e_i} - \mathcal{L}^0))} \left\| \mathcal{L}^0 + \sum_{i=1}^m u_i(\mathcal{L}^{e_i} - \mathcal{L}^0) \right\|^2 + \left\| e^{\tau\mathcal{L}^0}(\mathcal{L}^0)^2 + \sum_{i=1}^m u_i \left(e^{\tau\mathcal{L}^{e_i}}(\mathcal{L}^{e_i})^2 - e^{\tau\mathcal{L}^0}(\mathcal{L}^0)^2 \right) \right\|^2 \right\| \\
& \leq e^{\Delta t(\hat{u}\|\mathcal{L}^0\| + \sum_{i=1}^m |u_i|\|\mathcal{L}^{e_i}\|)} \left(\hat{u}\|\mathcal{L}^0\| + \sum_{i=1}^m |u_i|\|\mathcal{L}^{e_i}\| \right)^2 + \hat{u}e^{\Delta t\|\mathcal{L}^0\|} \|\mathcal{L}^0\|^2 + \sum_{i=1}^m |u_i|e^{\Delta t\|\mathcal{L}^{e_i}\|} \|\mathcal{L}^{e_i}\|^2 =: 2c_1
\end{aligned} \tag{28}$$

with $\hat{u} := \max_{u \in \mathbb{U}} |1 - \sum_{i=1}^m u_i|$. The constant c_1 is finite for a compact set \mathbb{U} of control actions. Hence, we have $\|h(\Delta t)\| \leq \Delta t^2 c_1 < \infty$. The terms $\|\mathcal{L}^{\bar{u}}\|$ with $\bar{u} \in \{0, e_1, \dots, e_m\}$ can be further bounded in terms of the system dynamics. To see this, we plug in the definition of the operator norm of \mathcal{L} as a mapping from \mathbb{V} to \mathbb{V} in view of Assumption 2.1, where we endow the finite-dimensional subspace \mathbb{V} of $L^2(X)$ with the L^2 -norm. W.l.o.g. the basis elements are scaled such that $\|\phi_\ell\|_{L^2(X)} = 1$, $\ell \in [0 : N]$, holds. Then, we obtain

$$\|\mathcal{L}^0\| = \sup_{\substack{\varphi \in \mathbb{V}, \\ \|\varphi\|_{L^2} = 1}} \|\nabla \varphi(\cdot)^\top f(\cdot)\|_{L^2(X)} = \sup_{\ell \in [0:N]} \|\nabla \phi_\ell(\cdot)^\top f(\cdot)\|_{L^2(X)} \leq \sup_{\ell \in [0:N]} \|\nabla \phi_\ell\|_{L^2(X)} \|f\|_{L^2(X)} \tag{29}$$

and, analogously, $\|\mathcal{L}^{e_i}\| \leq \sup_{\ell \in [0:N]} \|\nabla \phi_\ell\|_{L^2(X)} \|f + g_i\|_{L^2(X)}$, $i \in [m]$.

For an estimate on the second term in (26), we again use the Taylor expansion (27), the triangle inequality, and the notation and arguments used to derive Inequality (29) to get the estimate

$$\begin{aligned}
& \frac{2\|h(\Delta t)\Phi(0)\|}{\Delta t^2} \\
& \leq \underbrace{\left(e^{\Delta t(\hat{u}\|\mathcal{L}^0\| + \sum_{i=1}^m |u_i|\|\mathcal{L}^{e_i}\|)} \left(\hat{u}\|\mathcal{L}^0\| + \sum_{i=1}^m |u_i|\|\mathcal{L}^{e_i}\| \right) \right)}_{=: \tilde{c}} \left\| \left(1 - \sum_{i=1}^m u_i \right) \underbrace{\mathcal{L}^0 \Phi(0)}_{=0} + \sum_{i=1}^m u_i \underbrace{\mathcal{L}^{e_i} \Phi(0)}_{=\mathcal{L}_{21}^{e_i}} \right\| \\
& \quad + \left\| \left(\left(1 - \sum_{i=1}^m u_i \right) e^{\tau\mathcal{L}^0} \mathcal{L}^0 \right) \underbrace{\mathcal{L}^0 \Phi(0)}_{=0} \right\| + \left\| \sum_{i=1}^m u_i e^{\tau\mathcal{L}^{e_i}} (\mathcal{L}^{e_i})^2 \Phi(0) \right\| \\
& \leq \tilde{c} \left\| [\mathcal{L}_{21}^{e_1} \ \dots \ \mathcal{L}_{21}^{e_m}] \right\| \|u\| + \left\| [e^{\tau\mathcal{L}^{e_1}} (\mathcal{L}^{e_1})^2 \Phi(0) \ \dots \ e^{\tau\mathcal{L}^{e_m}} (\mathcal{L}^{e_m})^2 \Phi(0)] \right\| \|u\| \\
& \leq \tilde{c} \sqrt{\sum_{i=1}^m \|\mathcal{L}_{21}^{e_i}\|^2} \|u\| + \sqrt{\sum_{i=1}^m (e^{\Delta t\|\mathcal{L}^{e_i}\|} \|\mathcal{L}_{22}^{e_i}\| \|\mathcal{L}_{21}^{e_i}\|)^2} \|u\| \\
& \leq \tilde{c} \sqrt{m} \|\mathcal{L}_{21}^*\| \|u\| + \sqrt{m} e^{\Delta t\|\mathcal{L}^*\|} \|\mathcal{L}_{22}^*\| \|\mathcal{L}_{21}^*\| \|u\| =: 2\sqrt{m}c_2 \|u\|
\end{aligned} \tag{30}$$

using $(\mathcal{L}^{e_i})^2 \Phi(0) = \mathcal{L}_{22}^{e_i} \mathcal{L}_{21}^{e_i}$, the notations $\|\mathcal{L}_{21}^*\| := \max_{i=1}^m \|\mathcal{L}_{21}^{e_i}\|$, $\|\mathcal{L}_{22}^*\| := \max_{i=1}^m \|\mathcal{L}_{22}^{e_i}\|$, and $\|\mathcal{L}^*\| := \max_{i=1}^m \|\mathcal{L}^{e_i}\|$, respectively. Thus, we have $\|h(\Delta t)\Phi(0)\| \leq \Delta t^2 \sqrt{m}c_2 \|u\|$.

Hence, combining the two derived estimates (28) and (30) yields $\|\xi(x, u)\| \leq \Delta t^2 (c_1 \|\Phi(x) - \Phi(0)\| + \sqrt{m}c_2 \|u\|)$, i.e., the desired inequality. \square

Here, we emphasize that the constants c_1, c_2 in Lemma A.1 can be computed if, e.g., a bound on the L^2 -norm of the system dynamics is given.

2) *Data-driven surrogate of the bilinear representation of the Koopman operator:* Next, we approximate the bilinear representation of the Koopman operator by its respective data-driven estimates. To this end, we consider the data-driven surrogate model

$$\begin{aligned}\Phi(x_{k+1}) &= \mathcal{K}_{\Delta t, d}^u \Phi(x_k) + \xi(x_k, u_k) + \eta(x_k, u_k) \\ &= \mathcal{K}_{\Delta t, d}^0 \Phi(x_k) + \sum_{i=1}^m u_{k,i} (\mathcal{K}_{\Delta t, d}^{e_i} - \mathcal{K}_{\Delta t, d}^0) \Phi(x_k) + \xi(x_k, u_k) + \eta(x_k, u_k)\end{aligned}$$

corresponding to (12), where

$$\begin{aligned}\eta(x, u) &= \left(\mathcal{K}_{\Delta t}^0 \Phi(x) + \sum_{i=1}^m u_i (\mathcal{K}_{\Delta t}^{e_i} - \mathcal{K}_{\Delta t}^0) \Phi(x) \right) - \left(\mathcal{K}_{\Delta t, d}^0 \Phi(x) + \sum_{i=1}^m u_i (\mathcal{K}_{\Delta t, d}^{e_i} - \mathcal{K}_{\Delta t, d}^0) \Phi(x) \right) \\ &= \left((\mathcal{K}_{\Delta t}^0 - \mathcal{K}_{\Delta t, d}^0) + \sum_{i=1}^m u_i (\mathcal{K}_{\Delta t}^{e_i} - \mathcal{K}_{\Delta t, d}^{e_i}) + \sum_{i=1}^m u_i (\mathcal{K}_{\Delta t, d}^0 - \mathcal{K}_{\Delta t}^0) \right) \Phi(x)\end{aligned}\quad (31)$$

describes the estimation error due to the learning via sampled data. Before stating a bound on η , we first introduce the following proposition from the literature.

Proposition A.2 ([16, Thm. 14]). *Suppose that Assumption 2.1 holds and the data samples are i.i.d. Further, let an error bound $L_\eta > 0$ and a probabilistic tolerance $\delta \in (0, 1)$ be given. Then, there is an amount of data $d_0^{\bar{u}} = \mathcal{O}(1/\delta L_\eta^2)$ such that for all $d \geq d_0^{\bar{u}}$ we have the error bound*

$$\|\mathcal{K}_{\Delta t}^{\bar{u}} - \mathcal{K}_{\Delta t, d}^{\bar{u}}\| \leq L_\eta \quad (32)$$

for a fixed control input \bar{u} with probability $1 - \delta$.

Now, we show that the sampling error η in (31) satisfies the following proportional bound, where we exploit that Proposition A.2 can be applied for any $\bar{u} \in \{0, e_1, \dots, e_m\}$.

Lemma A.3. *Suppose that Assumption 2.1 holds and the data samples are i.i.d. Further, let an error bound $L_\eta > 0$ and a probabilistic tolerance $\delta \in (0, 1)$ be given. Then, there is an amount of data $d_0 = \mathcal{O}(1/\delta L_\eta^2)$ such that for all $d \geq d_0$ the approximation error η due to sampling of the Koopman operators $\mathcal{K}_{\Delta t, d}^{\bar{u}}$, $\bar{u} \in \{0, e_1, \dots, e_m\}$, based on the data satisfies the proportional bound*

$$\|\eta(x, u)\| \leq c_3 L_\eta \|\Phi(x) - \Phi(0)\| + \sqrt{m} L_\eta \|u\| \quad (33)$$

with probability $1 - \delta$, where $c_3 \in \mathbb{R}_+$ is defined in (34).

Proof. First, we apply Proposition A.2 for each $\bar{u} \in \{0, e_1, \dots, e_m\}$ and the given error bound L_η and probabilistic tolerance δ . This results in a necessary amount of data $d_0^{\bar{u}} \in \mathbb{N}$ for each fixed control input \bar{u} such that (32). We define the maximum of those necessary data lengths as $d_0 = \max\{d_0^0, d_0^{e_1}, \dots, d_0^{e_m}\}$ which ensures (32) for all data-driven estimates $\mathcal{K}_{\Delta t, d}^{\bar{u}}$ of the Koopman operator, where $\bar{u} \in \{0, e_1, \dots, e_m\}$.

Then, we recall the definition of the sampling error η in (31) and leverage $\Phi(x) = \Phi(x) - \Phi(0) + \Phi(0)$ to obtain

$$\begin{aligned}
\|\eta(x, u)\| &\leq \|(\mathcal{K}_{\Delta t}^0 - \mathcal{K}_{\Delta t, d}^0)(\Phi(x) - \Phi(0) + \Phi(0))\| \\
&\quad + \left\| \sum_{i=1}^m u_i (\mathcal{K}_{\Delta t}^{e_i} - \mathcal{K}_{\Delta t, d}^{e_i})(\Phi(x) - \Phi(0) + \Phi(0)) \right\| \\
&\quad + \left\| \sum_{i=1}^m u_i (\mathcal{K}_{\Delta t, d}^0 - \mathcal{K}_{\Delta t}^0)(\Phi(x) - \Phi(0) + \Phi(0)) \right\| \\
&\leq \|\mathcal{K}_{\Delta t}^0 - \mathcal{K}_{\Delta t, d}^0\| \|\Phi(x) - \Phi(0)\| + \|(\mathcal{K}_{\Delta t}^0 - \mathcal{K}_{\Delta t, d}^0)\Phi(0)\| \\
&\quad + \sum_{i=1}^m |u_i| \|\mathcal{K}_{\Delta t}^{e_i} - \mathcal{K}_{\Delta t, d}^{e_i}\| \|\Phi(x) - \Phi(0)\| \\
&\quad \quad + \left\| [(\mathcal{K}_{\Delta t}^{e_1})_{21} - (\mathcal{K}_{\Delta t, d}^{e_1})_{21} \quad \cdots \quad (\mathcal{K}_{\Delta t}^{e_m})_{21} - (\mathcal{K}_{\Delta t, d}^{e_m})_{21}] \right\| \|u\| \\
&\quad + \sum_{i=1}^m |u_i| \|\mathcal{K}_{\Delta t, d}^0 - \mathcal{K}_{\Delta t}^0\| \|\Phi(x) - \Phi(0)\| + \left\| \sum_{i=1}^m u_i (\mathcal{K}_{\Delta t, d}^0 - \mathcal{K}_{\Delta t}^0)\Phi(0) \right\|.
\end{aligned}$$

Next, we exploit $(\mathcal{K}_{\Delta t}^0 - \mathcal{K}_{\Delta t, d}^0)\Phi(0) = 0$ due to the structure of the Koopman operator in (8) and its data-driven approximate in (9), $\|\mathcal{K}_{\Delta t}^{\bar{u}} - \mathcal{K}_{\Delta t, d}^{\bar{u}}\| \leq L_\eta$ for $\bar{u} \in \{0, e_1, \dots, e_m\}$ according to (32), and

$$\begin{aligned}
\left\| [(\mathcal{K}_{\Delta t}^{e_1})_{21} - (\mathcal{K}_{\Delta t, d}^{e_1})_{21} \quad \cdots \quad (\mathcal{K}_{\Delta t}^{e_m})_{21} - (\mathcal{K}_{\Delta t, d}^{e_m})_{21}] \right\| &\leq \sqrt{\sum_{i=1}^m \|(\mathcal{K}_{\Delta t}^{e_i})_{21} - (\mathcal{K}_{\Delta t, d}^{e_i})_{21}\|^2} \\
&\leq \sqrt{\sum_{i=1}^m \|\mathcal{K}_{\Delta t}^{e_i} - \mathcal{K}_{\Delta t, d}^{e_i}\|^2},
\end{aligned}$$

which results in (33) with

$$c_3 = \left(1 + 2 \max_{u \in \mathbb{U}} \sum_{i=1}^m |u_i| \right). \quad (34)$$

This completes the proof. \square

Again, we emphasize that the constant c_3 in Lemma A.3 can be evaluated for a given set \mathbb{U} .

Now we can prove Theorem 3.1.

Proof (Theorem 3.1). This is a direct consequence of Lemma A.1 and Lemma A.3. We observe $(\mathcal{K}_{\Delta t}^u - \mathcal{K}_{\Delta t, d}^u)\Phi(x) = \xi(x, u) + \eta(x, u)$ and use the estimates in (25) and (33) to deduce

$$\begin{aligned}
\|(\mathcal{K}_{\Delta t}^u - \mathcal{K}_{\Delta t, d}^u)\Phi(x)\| &\leq \|\xi(x, u)\| + \|\eta(x, u)\| \\
&\leq (\Delta t^2 c_1 + c_3) \|\Phi(x) - \Phi(0)\| + \sqrt{m}(\Delta t^2 c_2 + L_\eta) \|u\|.
\end{aligned}$$

Then, defining

$$c_x = \Delta t^2 c_1 + c_3 L_\eta \quad \text{and} \quad c_u = \sqrt{m}(\Delta t^2 c_2 + L_\eta). \quad (35)$$

results in (13). In view of Lemma A.3, and for any probabilistic tolerance $\delta \in (0, 1)$, the constant L_η is of order $L_\eta = \mathcal{O}(1/\sqrt{\delta d_0})$ which implies the claim $c_x, c_u = \mathcal{O}(1/\sqrt{\delta d_0} + \Delta t^2)$. \square

B. Proof of Theorem 4.1

In the following, we prove Theorem 4.1 guaranteeing safe operation by exponential stability of the sampled nonlinear system (6) with the feedback control law (17). To this end, we first observe that the inclusion of the constant observable $\phi_0 \equiv 1$ and the thereof resulting structure of the Koopman operator (8) and its data-driven approximates (9) allows the simplification of the data-driven surrogate model

$$\Phi(x_{k+1}) = \mathcal{K}_{\Delta t, d}^u \Phi(x) + (\mathcal{K}_{\Delta t}^u - \mathcal{K}_{\Delta t, d}^u) \Phi(x) = \mathcal{K}_{\Delta t, d}^0 \Phi(x_k) + \sum_{i=1}^m u_{k,i} (\mathcal{K}_{\Delta t, d}^{e_i} - \mathcal{K}_{\Delta t, d}^0) \Phi(x_k) + \zeta(x_k, u_k)$$

with $\zeta := (\mathcal{K}_{\Delta t, d}^u - \mathcal{K}_{\Delta t}^u) \Phi(x)$. In particular, we observe that the first element of the learning error ζ is zero and, thus, $\|\zeta(x, u)\| = \|\hat{\zeta}(x, u)\|$ with $\hat{\zeta}(x, u) := [0_{N \times 1} \quad I_N] \zeta(x, u)$. Further, we exploit the structure in (8), (9) to deduce the lifted system representation

$$\begin{aligned} \hat{\Phi}(x_{k+1}) &= A \hat{\Phi}(x_k) + B_0 u_k + \sum_{i=1}^m (u_k)_i (\hat{B}_i - A) \hat{\Phi}(x_k) + \hat{\zeta}(x, u) \\ &= A \hat{\Phi}(x_k) + B_0 u_k + \tilde{B} (u_k \otimes \hat{\Phi}(x_k)) + \hat{\zeta}(x, u) \end{aligned} \quad (36)$$

with $B_0 = [B_{0,1} \quad \dots \quad B_{0,m}]$ and $\tilde{B} = [\hat{B}_1 - A \quad \dots \quad \hat{B}_m - A]$. Here, we use the reduced observable function $\hat{\Phi}(x) = [0_{N \times 1} \quad I_N] \Phi(x)$, where we removed the constant observable $\phi_0 \equiv 1$ such that $\hat{\Phi}(0) = 0$. According to the presented learning framework in Theorem 3.1, the reduced learning error $\hat{\zeta}(x, u)$ satisfies

$$\|\hat{\zeta}(x, u)\| = \|\zeta(x, u)\| \leq c_x \|\Phi(x) - \Phi(0)\| + c_u \|u\| = c_x \|\hat{\Phi}(x)\| + c_u \|u\| \quad (37)$$

for all $x \in \mathbb{X}$ and $u \in \mathbb{U}$.

Inspired by the controller designs in [18], [33], [34], we view (36) as an uncertain bilinear system with uncertainty $\hat{\zeta}(x, u)$. In particular, we use linear robust control techniques to cope with the uncertainty via convex optimization. More precisely, we define the remainder $\varepsilon : \mathbb{R}^N \times \mathbb{R}^m \rightarrow \mathbb{R}^N$ depending on the lifted state as

$$\varepsilon(v_1, v_2) = \hat{\zeta}([I_n \quad 0_{n \times N-n}] v_1, v_2). \quad (38)$$

According to the learning error bound (37), ε satisfies

$$\|\varepsilon(\hat{\Phi}(x), u)\| = \|\zeta(x, u)\| \leq c_x \|\hat{\Phi}(x)\| + c_u \|u\| \quad (39)$$

for all $x \in \mathbb{X}$ and $u \in \mathbb{U}$. To handle the nonlinear term $(u \otimes \hat{\Phi}(x))$, we introduce an artificial uncertainty $\psi \in \Delta_\Phi$ over-approximating $\hat{\Phi}(x)$. This uncertainty needs to be bounded, i.e., we ensure $\hat{\Phi}(x) \in \Delta_\Phi$ for all times. Then, we stabilize

$$\hat{\Phi}(x_{k+1}) = A \hat{\Phi}(x_k) + B_0 u_k + \tilde{B} (I_m \otimes \psi) u_k + \varepsilon(\hat{\Phi}(x), u)$$

for all $\psi \in \Delta_\Phi$ and perturbation functions ε satisfying (39) for all $x \in \mathbb{X}, u \in \mathbb{U}$. Setting $A_K = A + B_0 K$, $B_{K_w} = \tilde{B} + B_0 K_w$, and substituting the input by the feedback $u = \mu_\psi(x) = K \hat{\Phi}(x) + K_w (I_m \otimes \psi) \mu_\psi(x)$, we obtain the corresponding closed-loop system

$$\hat{\Phi}(x_{k+1}) = A_K \hat{\Phi}(x_k) + B_{K_w} (I_m \otimes \psi) \mu_\psi(x) + \varepsilon(\hat{\Phi}(x), \mu_\psi(x)) \quad (40)$$

with $\psi \in \Delta_\Phi$ and ε satisfying (39) for all $x \in \mathbb{X}$.

The remainder of the proof of Theorem 4.1 proceeds similarly to [18, Thm. 6] with the key difference of discrete vs. continuous time, and it is included in the following for completeness.

Proof. The presented proof is separated into two parts. First, we show that all $x \in \mathcal{X}_{\text{SOR}}$ satisfy $\hat{\Phi}(x) \in \Delta_\Phi$. Second, we conclude safe operation in \mathcal{X}_{SOR} by positive invariance of \mathcal{X}_{SOR} together with exponential stability of the sampled closed-loop system (6) for all $\hat{x} \in \mathcal{X}_{\text{SOR}}$.

Part I: $x \in \mathcal{X}_{\text{SOR}}$ implies $\hat{\Phi}(x) \in \Delta_\Phi$: In order to represent the lifted dynamics via (40), we require $\hat{\Phi}(x) \in \Delta_\Phi$ for all times. To this end, we exploit that

$$\begin{aligned} 0 &\succcurlyeq \frac{1}{\nu} \begin{bmatrix} \nu \tilde{R}_z - 1 & -\nu \tilde{S}_z^\top \\ -\nu \tilde{S}_z & \nu \tilde{Q}_z + P \end{bmatrix} = \begin{bmatrix} \tilde{R}_z & -\tilde{S}_z^\top \\ -\tilde{S}_z & \tilde{Q}_z \end{bmatrix} + \frac{1}{\nu} \begin{bmatrix} -1 & 0 \\ 0 & P \end{bmatrix} \\ &= \begin{bmatrix} 0 & I \\ -1 & 0 \end{bmatrix}^\top \begin{bmatrix} \tilde{Q}_z & \tilde{S}_z \\ \tilde{S}_z^\top & \tilde{R}_z \end{bmatrix} \begin{bmatrix} 0 & I \\ -1 & 0 \end{bmatrix} + \begin{bmatrix} 1 & 0 \\ 0 & -I \end{bmatrix}^\top \begin{bmatrix} -\frac{1}{\nu} & 0 \\ 0 & \frac{1}{\nu} P \end{bmatrix} \begin{bmatrix} 1 & 0 \\ 0 & -I \end{bmatrix} \end{aligned}$$

is equivalent to (16) after dividing the inequality by ν . We rewrite this inequality as

$$\begin{bmatrix} 0 & I \\ -I & 0 \\ I & 0 \\ 0 & -I \end{bmatrix}^\top \begin{bmatrix} \tilde{Q}_z & \tilde{S}_z & 0 & 0 \\ \tilde{S}_z^\top & \tilde{R}_z & 0 & 0 \\ 0 & 0 & -\frac{1}{\nu} & 0 \\ 0 & 0 & 0 & \frac{1}{\nu} P \end{bmatrix} \begin{bmatrix} 0 & I \\ -1 & 0 \\ 1 & 0 \\ 0 & -I \end{bmatrix} \preceq 0$$

and apply the dualization lemma [44, Lm. 4.9]. As a consequence, we obtain

$$\begin{bmatrix} I & 0 \\ 0 & 1 \\ 0 & 1 \\ I & 0 \end{bmatrix}^\top \begin{bmatrix} Q_z & S_z & 0 & 0 \\ S_z^\top & R_z & 0 & 0 \\ 0 & 0 & -\nu & 0 \\ 0 & 0 & 0 & \nu P^{-1} \end{bmatrix} \begin{bmatrix} I & 0 \\ 0 & 1 \\ 0 & 1 \\ I & 0 \end{bmatrix} \preceq 0,$$

i.e.,

$$\begin{bmatrix} Q_z & S_z \\ S_z^\top & R_z \end{bmatrix} - \nu \begin{bmatrix} -P^{-1} & 0 \\ 0 & 1 \end{bmatrix} \succeq 0.$$

Hence, we recall the definition of Δ_Φ in (14) and deduce $\hat{\Phi}(x) \in \Delta_\Phi$ for all $x \in \mathcal{X}_{\text{SOR}}$ by the multiplication from left and right by $[\hat{\Phi}(x)^\top \ 1]^\top$ and its transpose, respectively, for $x \in \mathcal{X}_{\text{SOR}}$ (cf. the S-procedure [44], [45]).

Part II: Safe operation by positive invariance of \mathcal{X}_{SOR} and exponential stability: In the following, we show $x_+ \in \mathcal{X}_{\text{SOR}}$ for all $x \in \mathcal{X}_{\text{SOR}}$ to conclude positive invariance of \mathcal{X}_{SOR} , where we use (x_+, x) as a short-hand notation for (x_{k+1}, x_k) . The obtained safe operating region \mathcal{X}_{SOR} will then result as a Lyapunov sublevel set, for which we define the Lyapunov function candidate $V(x) = \hat{\Phi}(x)^\top P^{-1} \hat{\Phi}(x)$, i.e., positive invariance can be inferred if $\Delta V(x) = V(x_+) - V(x) \leq 0$ for all $x \in \mathcal{X}_{\text{SOR}}$.

Recall $A_K = A + B_0 K$ and $B_{K_w} = \tilde{B} + B_0 K_w$. Then, the definitions $K = LP^{-1}$ and $K_w = L_w(\Lambda^{-1} \otimes I_N)$ together with twice applying the Schur complement (cf. [45]) to (15) yields

$$\begin{aligned} &\begin{bmatrix} P - \tau I_N & -B_{K_w}(\Lambda \otimes \tilde{S}_z) & 0 \\ -(\Lambda \otimes \tilde{S}_z^\top) B_{K_w}^\top & H_{K_w} & -(\Lambda \otimes \tilde{S}_z^\top) \begin{bmatrix} 0 \\ K_w \end{bmatrix}^\top \\ 0 & -\begin{bmatrix} 0 \\ K_w \end{bmatrix} (\Lambda \otimes \tilde{S}_z) & 0.5\tau \begin{bmatrix} c_x^{-2} I_N & 0 \\ 0 & c_u^{-2} I_m \end{bmatrix} \end{bmatrix} - \begin{bmatrix} A_K \\ K \\ I \\ K \end{bmatrix} P \begin{bmatrix} A_K \\ K \\ I \\ K \end{bmatrix}^\top \\ &\quad + \begin{bmatrix} B_{K_w}(\Lambda \otimes I_N) \\ K_w(\Lambda \otimes I_N) \\ 0 \\ -K_w(\Lambda \otimes I_N) \end{bmatrix} (\Lambda^{-1} \otimes \tilde{Q}_z) \begin{bmatrix} B_{K_w}(\Lambda \otimes I_N) \\ K_w(\Lambda \otimes I_N) \\ 0 \\ -K_w(\Lambda \otimes I_N) \end{bmatrix}^\top \succcurlyeq 0, \quad (41) \end{aligned}$$

where $H_{K_w} = (\Lambda \otimes \tilde{R}_z) - K_w(\Lambda \otimes \tilde{S}_z) - (\Lambda \otimes \tilde{S}_z^\top) K_w^\top$. We split the obtained matrix in three parts which we factor as

$$\begin{bmatrix} P & 0 & 0 \\ 0 & 0 & 0 \\ 0 & 0 & 0 \end{bmatrix} - \begin{bmatrix} A_K \\ K \\ I \\ K \end{bmatrix} P \begin{bmatrix} A_K \\ K \\ I \\ K \end{bmatrix}^\top = \begin{bmatrix} A_K & -I \\ K & 0 \\ I & 0 \end{bmatrix} \begin{bmatrix} -P & 0 \\ 0 & P \end{bmatrix} \begin{bmatrix} A_K & -I \\ K & 0 \\ I & 0 \end{bmatrix}^\top,$$

$$\begin{aligned}
& \begin{bmatrix} 0 & -B_{K_w}(\Lambda \otimes \tilde{S}_z) & 0 \\ -(\Lambda \otimes \tilde{S}_z^\top)B_{K_w}^\top & H_{K_w} & -(\Lambda \otimes \tilde{S}_z^\top) \begin{bmatrix} 0 \\ K_w \end{bmatrix}^\top \\ 0 & -\begin{bmatrix} 0 \\ K_w \end{bmatrix}(\Lambda \otimes \tilde{S}_z) & 0 \end{bmatrix} + \begin{bmatrix} B_{K_w} \\ K_w \\ -\begin{bmatrix} 0 \\ K_w \end{bmatrix} \end{bmatrix} (\Lambda \otimes \tilde{Q}_z) \begin{bmatrix} B_{K_w} \\ K_w \\ -\begin{bmatrix} 0 \\ K_w \end{bmatrix} \end{bmatrix}^\top \\
& = \begin{bmatrix} B_{K_w} & 0 \\ K_w & -I \\ \begin{bmatrix} 0 \\ K_w \end{bmatrix} & 0 \end{bmatrix} \begin{bmatrix} \Lambda \otimes \tilde{Q}_z & \Lambda \otimes \tilde{S}_z \\ \Lambda \otimes \tilde{S}_z^\top & \Lambda \otimes \tilde{R}_z \end{bmatrix} \begin{bmatrix} B_{K_w} & 0 \\ K_w & -I \\ \begin{bmatrix} 0 \\ K_w \end{bmatrix} & 0 \end{bmatrix}^\top,
\end{aligned}$$

and

$$\begin{bmatrix} -\tau I_N & 0 & 0 \\ 0 & 0 & 0 \\ 0 & 0 & 0.5\tau \begin{bmatrix} c_x^{-2} I_N & 0 \\ 0 & c_u^{-2} I_m \end{bmatrix} \end{bmatrix} = \tau \begin{bmatrix} I & 0 \\ 0 & 0 \\ 0 & -I \end{bmatrix} \Pi_r^{-1} \begin{bmatrix} I & 0 \\ 0 & 0 \\ 0 & -I \end{bmatrix}^\top$$

with

$$\Pi_r = \begin{bmatrix} -I_N & 0 \\ 0 & 2 \begin{bmatrix} c_x^2 I_N & 0 \\ 0 & c_u^2 I_m \end{bmatrix} \end{bmatrix}, \quad \Pi_r^{-1} = \begin{bmatrix} -I_N & 0 \\ 0 & 0.5 \begin{bmatrix} c_x^{-2} I_N & 0 \\ 0 & c_u^{-2} I_m \end{bmatrix} \end{bmatrix}.$$

This allows us to write (41) equivalently as

$$\begin{bmatrix} A_K^\top & K^\top & \begin{bmatrix} I \\ K \end{bmatrix}^\top \\ -I & 0 & 0 \\ \hline B_{K_w}^\top & K_w^\top & \begin{bmatrix} 0 \\ K_w \end{bmatrix}^\top \\ 0 & -I & 0 \\ \hline I & 0 & 0 \\ 0 & 0 & -I \end{bmatrix}^\top \begin{bmatrix} -P & 0 & 0 & 0 & 0 & 0 \\ 0 & P & 0 & 0 & 0 & 0 \\ \hline 0 & 0 & \Lambda \otimes \tilde{Q}_z & \Lambda \otimes \tilde{S}_z & 0 & 0 \\ 0 & 0 & \Lambda \otimes \tilde{S}_z^\top & \Lambda \otimes \tilde{R}_z & 0 & 0 \\ \hline 0 & 0 & 0 & 0 & \tau \Pi_r^{-1} & \\ 0 & 0 & 0 & 0 & & \end{bmatrix} \begin{bmatrix} A_K^\top & K^\top & \begin{bmatrix} I \\ K \end{bmatrix}^\top \\ -I & 0 & 0 \\ \hline B_{K_w}^\top & K_w^\top & \begin{bmatrix} 0 \\ K_w \end{bmatrix}^\top \\ 0 & -I & 0 \\ \hline I & 0 & 0 \\ 0 & 0 & -I \end{bmatrix} \succ 0.$$

Applying again the dualization lemma [44, Lm. 4.9] yields

$$\begin{bmatrix} I & 0 & 0 \\ A_K & B_{K_w} & I \\ \hline 0 & I & 0 \\ K & K_w & 0 \\ \hline 0 & 0 & I \\ \begin{bmatrix} I \\ K \end{bmatrix} & \begin{bmatrix} 0 \\ K_w \end{bmatrix} & 0 \end{bmatrix}^\top \begin{bmatrix} -P^{-1} & 0 & 0 & 0 & 0 & 0 \\ 0 & P^{-1} & 0 & 0 & 0 & 0 \\ \hline 0 & 0 & \Lambda^{-1} \otimes Q_z & \Lambda^{-1} \otimes S_z & 0 & 0 \\ 0 & 0 & \Lambda^{-1} \otimes S_z^\top & \Lambda^{-1} \otimes R_z & 0 & 0 \\ \hline 0 & 0 & 0 & 0 & \tau^{-1} \Pi_r & \\ 0 & 0 & 0 & 0 & & \end{bmatrix} \begin{bmatrix} I & 0 & 0 \\ A_K & B_{K_w} & I \\ \hline 0 & I & 0 \\ K & K_w & 0 \\ \hline 0 & 0 & I \\ \begin{bmatrix} I \\ K \end{bmatrix} & \begin{bmatrix} 0 \\ K_w \end{bmatrix} & 0 \end{bmatrix} \prec 0, \quad (42)$$

where we refer to the discussion in [44, Sec. 8.1.2] for details on how to build the outer matrices and exploit

$$\begin{bmatrix} \Lambda \otimes \tilde{Q}_z & \Lambda \otimes \tilde{S}_z \\ \Lambda \otimes \tilde{S}_z^\top & \Lambda \otimes \tilde{R}_z \end{bmatrix}^{-1} = \begin{bmatrix} \Lambda^{-1} \otimes Q_z & \Lambda^{-1} \otimes S_z \\ \Lambda^{-1} \otimes S_z^\top & \Lambda^{-1} \otimes R_z \end{bmatrix},$$

according to [34, Thm. 4 (proof)]. Then, we multiply (42) from the left and from the right by

$$\begin{bmatrix} \hat{\Phi}(x)^\top & (\mu_\psi(x) \otimes \psi)^\top & \varepsilon(\hat{\Phi}(x), \mu_\psi(x))^\top \end{bmatrix}^\top$$

and its transpose, respectively, where $x \in \mathcal{X}_{\text{SOR}}$, $\mu_\psi(x) = K\hat{\Phi}(x) + K_w(\mu_\psi(x) \otimes \psi)$, $\psi \in \Delta_\Phi$, and $\varepsilon(\hat{\Phi}(x), \mu_\psi(x))$ satisfies (39). This results in

$$\begin{aligned} [\star]^\top \begin{bmatrix} -P^{-1} & 0 \\ 0 & P^{-1} \end{bmatrix} \begin{bmatrix} \hat{\Phi}(x) \\ A_K\hat{\Phi}(x) + B_{K_w}(\mu_\psi(x) \otimes \psi) + \varepsilon(\hat{\Phi}(x), \mu_\psi(x)) \end{bmatrix} \\ + [\star]^\top \begin{bmatrix} \Lambda^{-1} \otimes Q_z & \Lambda^{-1} \otimes S_z \\ \Lambda^{-1} \otimes S_z^\top & \Lambda^{-1} \otimes R_z \end{bmatrix} \begin{bmatrix} (I_m \otimes \psi)\mu_\psi(x) \\ K\hat{\Phi}(x) + K_w(\mu_\psi(x) \otimes \psi) \end{bmatrix} \\ + \tau^{-1} [\star]^\top \Pi_r \begin{bmatrix} \varepsilon(\hat{\Phi}(x), \mu_\psi(x)) \\ \hat{\Phi}(x) \\ K\hat{\Phi}(x) + K_w(\mu_\psi(x) \otimes \psi) \end{bmatrix} < 0. \quad (43) \end{aligned}$$

Here, the second summand of (43) is nonnegative as

$$\mu_\psi(x)^\top \begin{bmatrix} I_m \otimes \psi \\ I_m \end{bmatrix}^\top \begin{bmatrix} \Lambda^{-1} \otimes Q_z & \Lambda^{-1} \otimes S_z \\ \Lambda^{-1} \otimes S_z^\top & \Lambda^{-1} \otimes R_z \end{bmatrix} \begin{bmatrix} I_m \otimes \psi \\ I_m \end{bmatrix} \mu_\psi(x) \geq 0$$

for any $\psi \in \Delta_\Phi$ according to the definition of Δ_Φ in (14) with [34, Prop. 2]. Moreover, the last summand in (43) is nonnegative as

$$\begin{aligned} [\star]^\top \Pi_r \begin{bmatrix} \varepsilon(\hat{\Phi}(x), \mu_\psi(x)) \\ \hat{\Phi}(x) \\ K\hat{\Phi}(x) + K_w(\mu_\psi(x) \otimes \psi) \end{bmatrix} &= 2(c_x^2 \|\hat{\Phi}(x)\|^2 + c_u^2 \|\mu_\psi(x)\|^2) - \|\varepsilon(\hat{\Phi}(x), \mu_\psi(x))\|^2 \\ &\geq (c_x \|\hat{\Phi}(x)\| + c_u \|\mu_\psi(x)\|)^2 - \|\varepsilon(\hat{\Phi}(x), \mu_\psi(x))\|^2 \geq 0. \end{aligned}$$

Hence, we can write (43) as

$$0 > (\star)^\top P^{-1} \left(A_K\hat{\Phi}(x) + B_{K_w}(\mu_\psi(x) \otimes \psi) + \varepsilon(\hat{\Phi}(x), \mu_\psi(x)) \right) - \hat{\Phi}(x)^\top P^{-1} \hat{\Phi}(x) < 0 \quad (44)$$

if $x \in \mathcal{X}_{\text{SOR}} \setminus \{0\}$, $\psi \in \Delta_\Phi$, and if $\varepsilon(\hat{\Phi}(x), \mu_\psi(x))$ satisfies (39) (compare, again, with the S-procedure [44], [45]).

Now, we recall the Lyapunov candidate function $V(x) = \hat{\Phi}(x)^\top P^{-1} \hat{\Phi}(x)$ and verify its satisfaction of $V(0) = 0$ and

$$\begin{aligned} V(x) &\leq \sigma_{\max}(P^{-1}) \|\hat{\Phi}(x)\|^2 \leq \sigma_{\max}(P^{-1}) L_\Phi^2 \|x\|^2, \\ V(x) &\geq \sigma_{\min}(P^{-1}) \|\hat{\Phi}(x)\|^2 \geq \sigma_{\min}(P^{-1}) \|x\|^2 \end{aligned}$$

due to $\|\hat{\Phi}(x)\| = \|\Phi(x) - \Phi(0)\|$ and (5). Then, we substitute (40) in (44), i.e., we use $\hat{\Phi}(x_+) = A_K\hat{\Phi}(x) + B_{K_w}(\mu_\psi(x) \otimes \psi) + \varepsilon(\hat{\Phi}(x), \mu_\psi(x))$. This yields

$$\Delta V(x) = V(x_+) - V(x) = \hat{\Phi}(x_+)^\top P^{-1} \hat{\Phi}(x_+) - \hat{\Phi}(x)^\top P^{-1} \hat{\Phi}(x) < 0 \quad (45)$$

if $x \in \mathcal{X}_{\text{SOR}} \setminus \{0\}$, $\psi \in \Delta_\Phi$, and if $\varepsilon(\hat{\Phi}(x), \mu_\psi(x))$ satisfies (39). Hence, the controller $\mu_\psi(x) = K\hat{\Phi}(x) + K_w(\mu_\psi(x) \otimes \Delta_\Phi)$ guarantees (45) for solutions of the lifted system (40) if $x \in \mathcal{X}_{\text{SOR}} \setminus \{0\}$, $\psi \in \Delta_\Phi$, and if $\varepsilon(\hat{\Phi}(x), \mu_\psi(x))$ satisfies (39). As proven in Part I, we have $\hat{\Phi}(x) \in \Delta_\Phi$ for all $x \in \mathcal{X}_{\text{SOR}}$. Further, $\varepsilon(\hat{\Phi}(x), \mu(x)) = \hat{\zeta}(x, \mu(x))$ due to (38). Consequently, the controller

$$\mu(x) = \mu_{\psi=\hat{\Phi}(x)}(x) = K\hat{\Phi}(x) + K_w(I_m \otimes \hat{\Phi}(x))\mu(x) = (I - K_w(I_m \otimes \hat{\Phi}(x)))^{-1} K\hat{\Phi}(x)$$

renders \mathcal{X}_{SOR} positive invariant by guaranteeing (45) in particular for system (36) for all $x \in \mathcal{X}_{\text{SOR}} \setminus \{0\}$ if $\hat{\zeta}(x, \mu(x))$ satisfies (37). Moreover, we deduce robust exponential stability of (36) for all $x \in \mathcal{X}_{\text{SOR}}$ if $\hat{\zeta}(x, \mu(x))$ satisfies (37).

Finally, we exploit the certificates of SafEDMD in Theorem 3.1, i.e., we deduce that the data-driven surrogates $K_{\Delta t, d}^{\bar{u}}$, $\bar{u} \in \{0, e_1, \dots, e_m\}$, and the resulting learning error $\hat{\zeta}(x, \mu(x))$ of the certified learning scheme in Section 3 satisfy the obtained learning error bound (13) for a data length $d \geq d_0$ with probability $1 - \delta$. Hence, we conclude safe operation by exponential stability of the sampled nonlinear system (6) for all $x \in \mathcal{X}_{\text{SOR}}$ with probability $1 - \delta$. \square

C. Proof of Corollary 4.2

In the following, we prove the stability certificates in Corollary 4.2 for the continuous-time system (1) in closed loop with the sampling-based controller (18).

Proof. This is a direct consequence of Theorem 4.1, where we exploit similar arguments as in [35, Thm. 2.27] to infer stability guarantees for the continuous-time system (1) based on the sampled controller (18). In order to show the statement, we need the solutions of the sampled-data closed-loop system to be uniformly bounded over Δt as defined in [35, Def. 2.24], i.e., we have to show the existence of a \mathcal{K} -function⁴ γ such that for all $\hat{x} \in \mathcal{X}_{\text{SOR}}$, the solutions of the nonlinear system (1) satisfy

$$\|x(\tau; \hat{x}, \mu_s(x))\| \leq \gamma(\|\hat{x}\|) \quad (46)$$

for all $\tau \in [0, \Delta t]$. Note that the sampled controller $\mu_s(x)$ yields a constant value $\mu_s(x(\tau)) \equiv \bar{\mu} \in \mathbb{U}$ for $\tau \in [0, \Delta t]$. Thus, we observe

$$\|x(\tau; \hat{x}, \bar{\mu})\| \leq \max_{\bar{u} \in \mathbb{U}} \|x(\tau; \hat{x}, u)\| \stackrel{(5)}{\leq} \max_{\bar{u} \in \mathbb{U}} \|\Phi(x(\tau; \hat{x}, u)) - \Phi(0)\|$$

for all $\tau \in [0, \Delta t)$ with $u(t) \equiv \bar{u}$ on $[0, \Delta t)$. Further, recalling $\phi_0 \equiv 1$ and, hence, $\mathcal{K}_\tau^u \Phi(0) = \Phi(0)$, we deduce

$$\Phi(x(\tau; \hat{x}, u)) - \Phi(0) \stackrel{(2)}{=} \mathcal{K}_\tau^u \Phi(\hat{x}) - \mathcal{K}_\tau^u \Phi(0) = e^{\tau \mathcal{L}^{\bar{u}}} (\Phi(\hat{x}) - \Phi(0))$$

for all $\tau \in [0, \Delta t)$. Then,

$$\|x(\tau; \hat{x}, \bar{\mu})\| \leq e^{\Delta t \|\mathcal{L}^*\|} \|\Phi(\hat{x}) - \Phi(0)\| \stackrel{(5)}{\leq} e^{\Delta t \|\mathcal{L}^*\|} L_\Phi \|\hat{x}\|$$

where $\|\mathcal{L}^*\| := \max_{\bar{u} \in \mathbb{U}} \|\mathcal{L}^{\bar{u}}\|$. Hence, (46) holds for the linear function $\gamma(r) := cr$ with $c := e^{\Delta t \|\mathcal{L}^*\|} L_\Phi$. Moreover, exponential stability of the sampled system guarantees the existence of $C \geq 1$ and $\sigma \in (0, 1)$ such that $\|x(k\Delta t)\| \leq C\sigma^k \|\hat{x}\|$ holds for all $k \geq 0$, which corresponds to the \mathcal{KL} -function⁵ $\beta(r, k) = C\sigma^k r$. Hence, for any $t \in [k\Delta t, (k+1)\Delta t)$ with $k \geq 0$ we get

$$\|x(t; \hat{x}, \mu_s(x))\| \leq \gamma(\|x(k\Delta t; \hat{x}, \bar{\mu}_k)\|) \leq \gamma(\beta(\|\hat{x}\|, k)) \leq cC\sigma^k \|\hat{x}\| \leq \tilde{C}e^{-t\eta} \|\hat{x}\|$$

for $\bar{\mu}_k = \mu_s(x(k\Delta t))$ and with $\eta := -\ln(\sigma)\Delta t^{-1} > 0$ and $\tilde{C} := cC\sigma^{-1}$, i.e., exponential stability of the continuous-time closed-loop system. \square

⁴We denote the class of functions $\alpha : \mathbb{R}_{\geq 0} \rightarrow \mathbb{R}_{\geq 0}$, which are continuous, strictly increasing, and satisfy $\alpha(0) = 0$ by \mathcal{K} .

⁵A continuous function $\beta : \mathbb{R}_{\geq 0} \times \mathbb{R}_{\geq 0} \rightarrow \mathbb{R}_{\geq 0}$ belongs to class \mathcal{KL} if $\beta(\cdot, s) \in \mathcal{K}$ for each fixed s and $\beta(r, \cdot)$ is decreasing with $\lim_{s \rightarrow \infty} \beta(r, s) = 0$ for each fixed r .